

A knowledge-based model of civilization under climate change

Boris M. Dolgonosov

Haifa, Israel

E-mail: borismd31@gmail.com

Abstract

Civilization produces knowledge, which acts as the driving force of its development. A macro-model of civilization that accounts for the effect of knowledge production on population, energy consumption and environmental conditions is developed. The model includes dynamic equations for world population, amount of knowledge circulating in civilization, the share of fossil fuels in total energy consumption, atmospheric CO₂ concentration, and global mean surface temperature. Energy dissipation in knowledge production and direct loss of knowledge are taken into account. The model is calibrated using historical data for each variable. About 90 scenarios were calculated. It was shown that there are two control parameters – sensitivity of the population to temperature rise and coefficient of knowledge loss – which determine the future of civilization. In the two-dimensional space of these parameters, there is an area of sustainable development and an area of loss of stability. Calculations show that civilization is located just on the critical curve separating these areas, that is, at the edge of stability. A small deviation can ultimately lead either to a steady state of 10+ billion people or to the complete extinction of civilization. There are no intermediate steady states.

Keywords: world population; knowledge production; CO₂ emissions; temperature anomaly; sustainable development; loss of stability.

Highlights

Knowledge is the driving force behind the development of civilization.

Two parameters – temperature sensitivity and knowledge loss – determine civilization development.

In parametric space there exist areas of sustainable development and loss of stability.

Civilization is placed right on the critical curve separating stable and unstable areas.

Civilization eventually comes either to a steady state of 10+ billion or to extinction.

1. Introduction

Systematic environmental monitoring reveals global climate change associated with human impact (IPCC, 2013). The increase in global mean surface temperature due to the burning of fossil fuels and some associated processes has numerous negative consequences (Andrews et al., 2018) disrupting the existing human adaptation, which results in deceleration of population growth and may even lead to population decline in the near future. Environmental degradation directs scientific and technological research to reduce fossil fuel consumption, search for new energy sources and develop new environment-friendly technologies. A quantitative description of this system within the framework of a single model is advisable, which however is a difficult problem since it is necessary to combine heterogeneous processes – demographic, physical, technological and informational – and take into account their interaction.

Puliafito et al. (2008) proposed a system of coupled equations describing population dynamics, CO₂ emissions, energy consumption and gross domestic product based on an approach in which variables were regarded as separate species interacting as a prey-predator in accordance with the Lotka–Volterra equations. Taagepera (2014) studied the effects of technology and environmental carrying capacity on population growth. Stutz (2014) showed that consumption costs affect the elasticity of the carrying capacity over time. Miranda and Lima (2011) analyzed different approaches to population dynamics and concluded that the power-law model is applicable for the initial stages of the process, while the Allee logistic model can describe the whole process.

The combination of informational and demographic processes within a single model was first undertaken by Dolgonosov and Naidenov (2006), who examined the joint dynamics of knowledge and population. The model is based on the integral principle of least action as applied to the transition of civilization from one level of knowledge to a higher one. The model accounts for the limited resources of the planet, assuming that the environmental conditions are unchanged. However, if we want to describe the human impact on the environment, this assumption must be discarded. Another assumption was that the system accumulates knowledge without loss. But actually, one must keep in mind energy dissipation in knowledge production, and also not neglect the direct loss of knowledge. In order to connect physical processes related to CO₂ emissions and temperature rise (Archer et al., 2009; Joos et al. 2013) to this model, we also need to consider the possibility of technological improvements that lower environmental impact by reducing fossil fuel consumption. New technologies are developed using available

knowledge that is in active circulation and supported by real knowledge holders. Thus, we come to the concept of active knowledge (introduced by Wiig, 1993), which is used in our study.

A knowledge-based demographic model was considered by Akaev and Sadovnichii (2010), who modified Dolgonosov's (2009) model by including in it delays caused by achieving reproductive age, diffusion of core technologies, and the environmental response to anthropogenic load. Aral (2013, 2014) included an additional term in the modified model that describes the effect of temperature rise on population. The temperature in this model was regarded as an external factor; its change in time was taken from the well-known IPCC scenario allowing a temperature rise of 2°C (Solomon et al., 2007).

Dong et al. (2016) examined the relationship between population N and scientific and technological knowledge q based on an empirical approach. The authors tested several hypotheses regarding this relationship, one of which in our notation looks like this: $\dot{q} = w(q)N$, where $w(q) = aq$ is the per capita knowledge production. Okuducu and Aral (2017) considered five options for the function $w(q)$, including $w(q) = \text{constant}$ and a linear dependence $w(q) = aq + b$ with $a = b$. In our approach, we take $w(q) = \text{constant}$, which ensures compliance with the well-known hyperbolic law of population growth empirically discovered by von Foerster et al. (1960).

The objective of this work is to create a model that includes appropriate demographic, physical, technological and informational processes. To reduce complexity, we focus on creating a minimal model that considers dynamics on a global scale, thereby avoiding an increase in the number of parameters while preserving the features of the interaction between the processes.

2. Knowledge production and population dynamics

2.1. Dissipative dynamics

We have earlier studied the macro-model of civilization as a system that produces the knowledge necessary for survival (Dolgonosov, 2016). Knowledge is defined as a set of descriptions of objects and phenomena (declarative knowledge), as well as a set of process algorithms (procedural knowledge) (ten Berge, van Hezewijk, 1999); for a more detailed classification of knowledge, see Burgin (2017). Strictly speaking, the amount of knowledge is measured by the minimum amount of memory that is needed to store knowledge written in the

same language. However, in reality, knowledge is written in different languages without minimizing memory, so we have to deal with the actual amount of memory used.

Based on the least action principle in knowledge production, we have derived the equation of knowledge dynamics

$$\ddot{q} = k\dot{q}^2(1 - b\dot{q}) \quad (1)$$

where q is the knowledge amount, k is a growth coefficient, and b characterizes the inhibition of knowledge production due to environmental limitations. The inhibition factor b was shown to be a function of knowledge amount

$$b = b_s(1 - e^{-aq}), \quad (2)$$

where b_s is the inhibition coefficient, and a is the inhibition increment. Equation (1) applies to a system without knowledge loss. However, real civilization not only loses knowledge but also dissipates energy in knowledge production. The dissipation can be taken into account by introducing an additional term $-l\dot{q}$ in equation (1); namely

$$\ddot{q} = k\dot{q}^2(1 - b\dot{q}) - l\dot{q}, \quad (3)$$

where l is a dissipation factor.

Civilization generates knowledge with the rate

$$\dot{q} = wN, \quad (4)$$

where N is the population size, and w is the per capita knowledge production rate, which is considered constant as mentioned in Section 1. Substituting (4) in (3), we get a population dynamic equation

$$\dot{N} = kwN^2(1 - bwN) - lN \quad (5)$$

which depends, through its coefficients, on knowledge amount q .

The processing of historical population data shows (Dolgonosov, 2016) that population growth over the last thousand years up to the last quarter of the 20th century is well described by the equation $\dot{N} = kwN^2$ provided that k is constant (same as w), which leads to the familiar hyperbolic law (von Foerster et al., 1960).

Based on equations (3) and (4), we can trace the analogy with mechanics, which gives such a correspondence: q is coordinate, \dot{q} is velocity, N is momentum, and w^{-1} is mass. In the spirit of this analogy, the first term on the right in equation (5) is the difference between the driving force $\sim N^2$ (promoting population growth due to knowledge production) and the returning force $\sim N^3$ (inhibiting growth caused by environmental limitations), and the second term is the friction force $\sim N$ (decelerating growth owing to knowledge loss) associated with energy dissipation in a viscous medium.

2.2. The concept of active knowledge

The production of knowledge is accompanied by energy dissipation. There are also direct losses of knowledge caused by its obsolescence and knowledge holders' mortality. Only the active knowledge (Wiig, 1993) circulating in society determines the level of life-support technologies and thereby affects the population. This means that the inhibition factor b should depend on the amount of active knowledge Q , and not on all the knowledge q produced by civilization in its entire history. Then, instead of equation (2), we must write

$$b = b_s(1 - e^{-aQ}). \quad (6)$$

Knowledge remains active for a limited time. As the population grows, the knowledge lifespan τ increases, since a proportionately larger number of people can support knowledge. This can be written as

$$\tau = hN, \quad (7)$$

where h is a coefficient.

The balance of active knowledge consists of knowledge production at a rate of $\dot{q} = wN$ and its loss at a rate of Q/τ , which leads to the equation

$$\dot{Q} = wN - \frac{Q}{hN}. \quad (8)$$

A similar equation (in our notation) $\dot{Q} = wN - \lambda Q$, where Q is the amount of culture, was obtained by Ghirlanda et al. (2010), which examined the effect of cultural development on

population dynamics. The difference is that in the cited paper λ is a constant, whereas according to (8) we have the correspondence $\lambda = 1/(hN)$.

In equilibrium, equation (8) yields $Q = whN^2$, so the active knowledge amount is proportional to the population squared and becomes the larger, the higher the knowledge production rate w and the coefficient h . Equation (8) also shows that when civilization collapses and knowledge holders disappear ($N \rightarrow 0$), active knowledge also disappears ($Q \rightarrow 0$). Unlike the active knowledge Q , the cumulative amount of knowledge q produced by civilization increases monotonously as long as civilization exists, but if it collapses, q reaches a plateau

$$q_{\infty} = w \int_0^{\infty} N(t) dt \quad (9)$$

(Dolgonosov and Naidenov, 2006) and stays at this level. However, this knowledge is dead because there is no one to utilize it.

3. The effect of temperature rise

3.1. The dissipation factor

Environmental degradation holds back growth of knowledge production by increasing the dissipation factor l introduced in (3). This parameter depends on environmental conditions through a chain of causal relations: fossil fuel consumption – CO₂ emissions – temperature rise – dissipation increase.

On the other hand, the deterioration of environmental conditions induces the chain: knowledge increase – development of technology – reduction in fossil fuel consumption due to the transition to alternative energy sources – decrease in CO₂ emissions, temperature and energy dissipation.

Let us consider the temperature dependence of the dissipation factor l . As a generalized indicator of environmental conditions, we take global mean surface temperature, although there is an opinion that water scarcity is a critical factor (Parolari et al., 2015). However, most likely it is a secondary factor induced by global warming. As noted by Andrews et al. (2018), heat stress affects the workability and survivability of people, and the dependence of heat exposure on temperature is non-linear. Estimates show that with an increase in temperature by $\sim 2.5^{\circ}\text{C}$ above

the pre-industrial level about 1 billion people will suffer. The pre-industrial temperature is optimal in the sense that humanity has adapted to it, creating an appropriate life-support infrastructure. Deviations from the optimum will lead to increased energy consumption to maintain a comfortable temperature. Assuming that the dissipation factor is a smooth function of temperature, we can represent it in the vicinity of the optimum as a quadratic form

$$l = l_s \left(1 + \frac{\Delta T^2}{\sigma^2} \right), \quad (10)$$

where l_s is the dissipation coefficient, $\Delta T = T - T_0$ is the temperature anomaly, T and T_0 are the current temperature and the pre-industrial one, and σ may be called “temperature tolerance”.

3.2. Temperature anomaly

Temperature anomaly is proportional to the radiative forcing, which is a function of atmospheric CO₂ concentration. There are several expressions for this function (IPCC, 1990, Chap. 2), the simplest of which is the logarithmic law proposed by Wigley (1987) and leading to

$$\Delta T = \vartheta \ln \frac{C}{C_0}, \quad (11)$$

where C_0 and C are the pre-industrial and the current CO₂ concentrations, respectively, and ϑ is a temperature constant. Time series of mean surface temperature and atmospheric CO₂ concentration are known from the literature (NASA, 2016; IAC Switzerland, 2014; Scripps UCSD, 2017), which make it possible to find a relationship between temperature and CO₂ concentration. This relationship and its trend for 1880 – 2017 are depicted in Fig. 1. The comparison of the logarithmic regression in Fig. 1 with equation (11) gives

$$\vartheta = 3.3917 \text{ K}, \quad T_0 - \vartheta \ln C_0 = 267.59. \quad (12)$$

According to the historical data on carbon dioxide (IAC Switzerland, 2014), CO₂ concentration in 1650 is

$$C_0 = 276.41 \text{ ppm}. \quad (13)$$

Then, from (12) and (13), we get

$$T_0 = 286.66 \text{ K}. \quad (14)$$

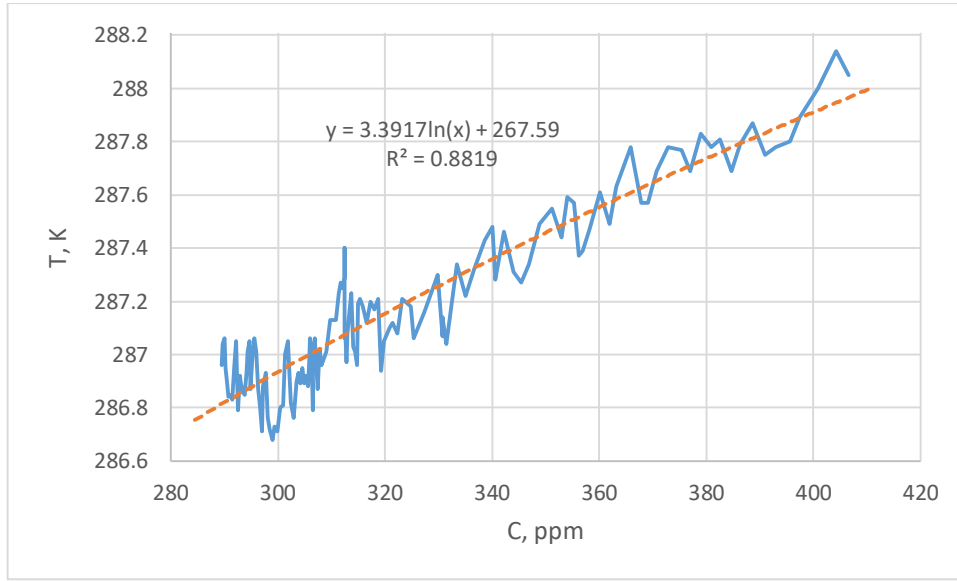


Fig. 1. Earth's mean surface temperature versus CO₂ concentration in the atmosphere. Data sources: temperature – [NASA, 2016](#); CO₂ – [IAC Switzerland, 2014](#); [Scripps UCSD, 2017](#).

3.3. Carbon dioxide emissions

Anthropogenic CO₂ emissions superimposed on natural atmospheric CO₂ fluctuations lead to an increase in CO₂ concentration as shown in Fig. 2 on a logarithmic scale for the period of 1650 – present. A polynomial approximation for $\ln C$ is also indicated there. This approximation is used below in model calibration (Section 5).

Carbon dioxide emissions from burning fossil fuels give an annual increase (ppm/year) in atmospheric CO₂

$$J = pE_C, \quad (15)$$

where E_C is the fossil fuel consumption (Gtoe/year, Gtoe = Giga tonne of oil equivalent), and p is the increase in CO₂ per unit of fuel burned (ppm/Gtoe). Coefficient p can be found using the dependence of CO₂ concentration on cumulative fuel consumption (Fig. 3). The regression in Fig. 3 indicates that

$$p = 0.2194 \text{ ppm/Gtoe}. \quad (16)$$

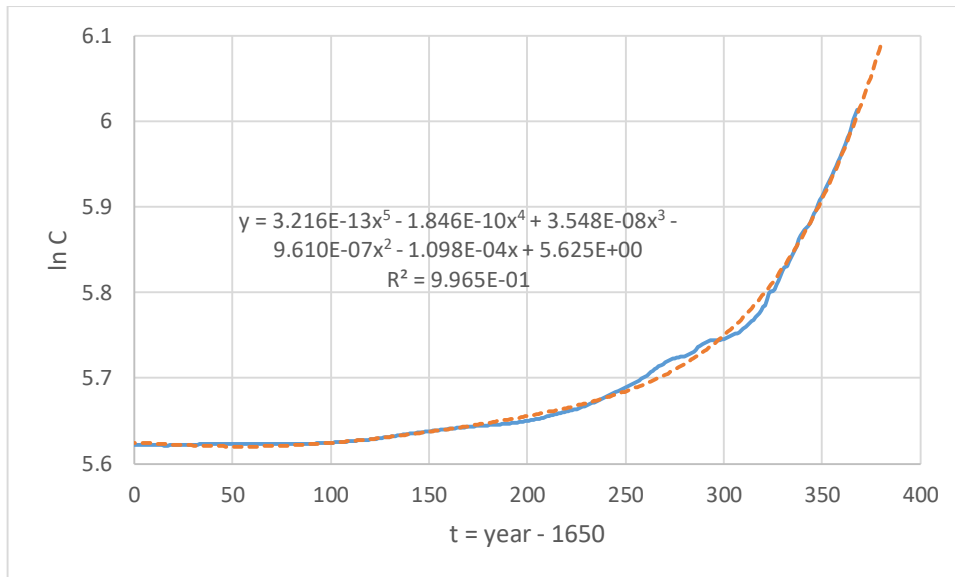


Fig. 2. The logarithm of CO₂ concentration (solid curve) and its polynomial approximation (dashed curve). Data sources: [IAC Switzerland, 2014](#); [Scripps UCSD, 2017](#).

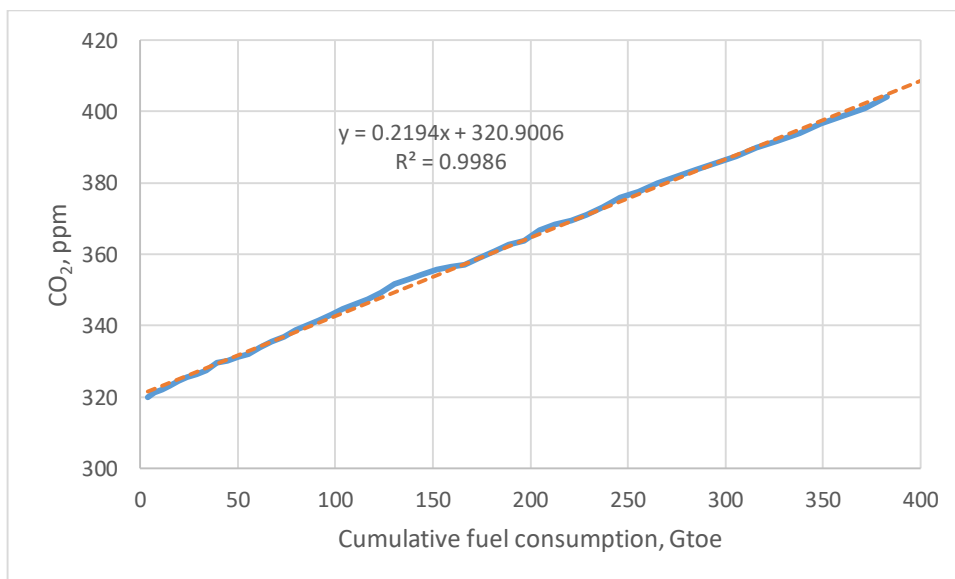


Fig. 3. Atmospheric CO₂ concentration versus cumulative fuel consumption. Data sources: CO₂ concentration – [IAC Switzerland, 2014](#); energy consumption and CO₂ emissions – [BP, 2018](#).

The kinetics of reducing CO₂ excess after its instantaneous pulse into the atmosphere was calculated using various models that describe the removal of CO₂ through land uptake, ocean invasion and silicate weathering ([Archer et al., 2009](#); [Joos et al. 2013](#)). The averaged aggregate kinetics of these processes depicted in Fig. 4 can be approximated by a power-law

$$G(t) = \left(1 + \frac{t}{\tau_c}\right)^{-g}, \quad g = 0.2350, \quad \tau_c = 2.30 \text{ year}, \quad (17)$$

where G is the share of CO₂ remaining in the atmosphere, t is the time after the CO₂ pulse. For $t \gg \tau_c$, we have the asymptotic law $G(t) \sim t^{-g}$.

Since CO₂ emissions occur continuously, CO₂ concentration in the atmosphere can be determined by the integral equation

$$C(t) = C_0 + \int_0^t J(\tau) G(t - \tau) d\tau. \quad (18)$$

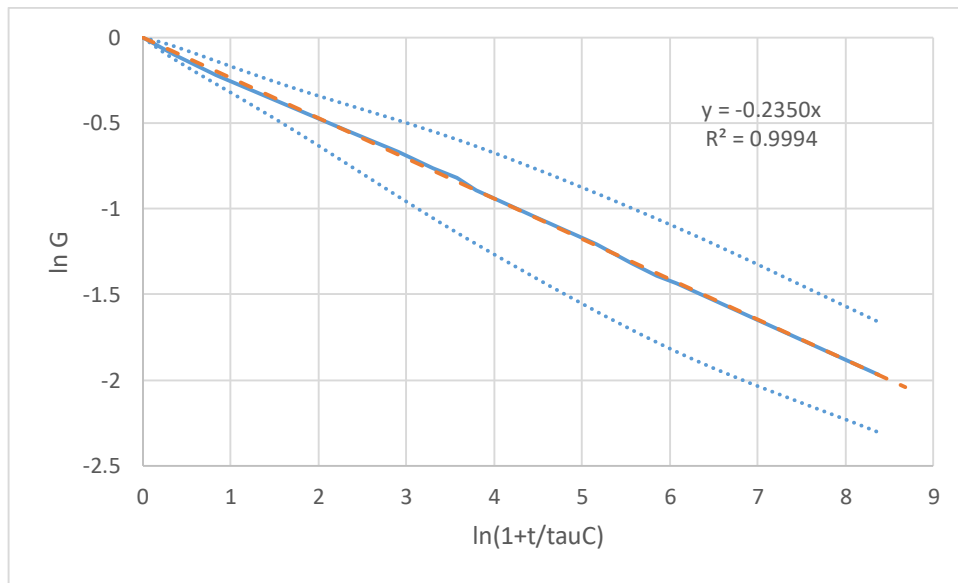


Fig. 4. The share of CO₂ pulse remaining in the atmosphere. The initial pulse is 100 GtC at zero moment. Solid curve: kinetics averaged across different models; dotted curves: uncertainty interval ± 2 stdev (for calculations on different models); dashed curve: calculations according to equation (17). Data sources: Joos et al., 2013; IPCC, 2013, Chap. 6.

3.4. The share of fossil fuels in total energy consumption

The relation between fossil fuel consumption E_C and total energy consumption E_{tot} is

$$E_C = f E_{\text{tot}}, \quad (19)$$

where f is the share of fossil fuels in total energy consumption; f depends on the amount of knowledge. As shown by Dolgonosov (2018), total energy consumption is a power-law function

of the population (Fig. 5)

$$E_{\text{tot}} = KN^d, \quad K = 0.6620, \quad d = 1.5, \quad R^2 = 0.9886, \quad (20)$$

where E_{tot} is measured in Gtoe/year and N in billions.

Factor f in equation (19) reflects the human impact on the environment. The accumulation of active knowledge can reduce this impact by phasing out fossil fuels in favor of alternative energy sources. The rate of impact reduction with knowledge growth directly depends on the impact magnitude and the knowledge amount that can be written as

$$f' = -2cQf, \quad (21)$$

where the prime is the derivative with respect to Q . A solution to this equation is

$$f = f_0 e^{-cQ^2}. \quad (22)$$

where f_0 and c are constants. From this formula it follows that with increasing knowledge, fossil fuel consumption decreases. However, if Q diminishes due to loss of knowledge, fuel consumption resumes its growth.

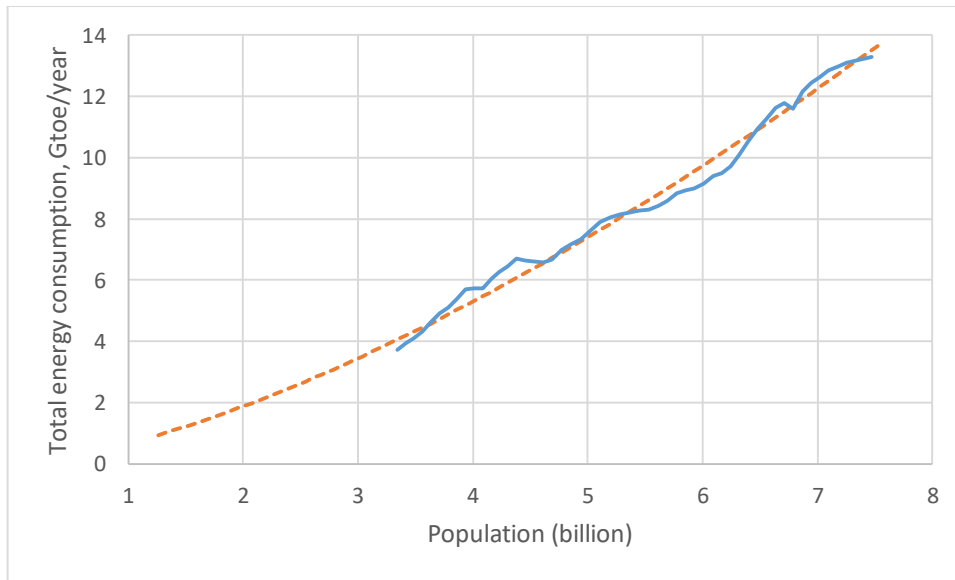


Fig. 5. Total energy consumption as a function of population. Solid curve: data. Dashed curve: trend according to equation (20). Data sources: energy consumption – [BP, 2018](#); population – [US Census Bureau, 2018](#).

4. Model

4.1. Model equations

Gathering the relationships obtained in the previous sections, we get a complete system of model equations:

active knowledge

$$\dot{Q} = wN - \frac{Q}{hN}; \quad (23)$$

world population

$$\dot{N} = kwN^2 \left(1 - b_s wN(1 - e^{-aQ})\right) - l_s N \left(1 + \frac{\Delta T^2}{\sigma^2}\right); \quad (24)$$

temperature anomaly

$$\Delta T = 9 \ln \frac{C}{C_0}; \quad (25)$$

atmospheric CO₂ concentration

$$C(t) = C_0 + pf_0 K \int_0^t N^d(\tau) e^{-cQ^2(\tau)} \left(1 + \frac{t-\tau}{\tau_c}\right)^{-g} d\tau. \quad (26)$$

Initial conditions:

$$Q(0) = Q_0, \quad N(0) = N_0, \quad (27)$$

where $t = 0$ corresponds to 1650. As shown by [Hilbert and Lopez \(2012a, 2012b\)](#), the amount of information increased by two orders of magnitude over a 21-year interval: from $0.4 \cdot 10^{13}$ Mbyte in 1986 to $30.5 \cdot 10^{13}$ Mbyte in 2007. An even greater difference should be expected when comparing the year 1650 with modernity. The same goes for knowledge, so we take the initial value $Q_0 = 0$.

4.2. Normalization

Normalization reduces the number of model parameters. Normalized variables x, y, z and u are defined as

$$t = \tau_s x, \quad Q = Q_s y, \quad N = N_s z, \quad C = C_0(1+u), \quad (28)$$

where the scale factors are

$$\tau_s = \frac{b_s}{k}, \quad Q_s = \frac{1}{k}, \quad N_s = \frac{1}{b_s w}. \quad (29)$$

Normalized equations:

$$y' = z - \frac{vy}{z}, \quad (30)$$

$$z' = z^2(1 - z(1 - e^{-\alpha y})) - \gamma z(1 + \beta^2 \ln^2(1+u)), \quad (31)$$

$$u(x) = \delta \int_0^x z^d(s) e^{-\eta y^2(s)} (1 + \varepsilon(x-s))^{-g} ds, \quad (32)$$

where the prime is the derivative with respect to x . Initial conditions:

$$y(0) = 0, \quad z(0) = z_0 = \frac{N_0}{N_s}. \quad (33)$$

Dimensionless parameters in equations (30) – (32) are defined as

$$\begin{aligned} \alpha &= aQ_s, \quad \beta = \frac{\vartheta}{\sigma}, \quad \gamma = l_s \tau_s, \quad \delta = \frac{f_0 p K}{C_0} N_s^d \tau_s, \\ \eta &= cQ_s^2, \quad \varepsilon = \frac{\tau_s}{\tau_C}, \quad v = \frac{\tau_s}{hN_s}. \end{aligned} \quad (34)$$

A brief description of the quantities used in the model (as well as in its calibration, see Section 5) is given in Table 1.

Table 1. Description of the main model variables, parameters, and related quantities

Notation	Unit	Description
<i>Main variables</i>		
N	billion	world population
C	ppm	CO ₂ concentration in the atmosphere
T	K	global mean surface temperature
Q	Mbook	active knowledge amount
t	year	time
f		share of fossil fuels in total energy consumption
<i>Initial values</i>		
N_0	billion	initial population
C_0	ppm	pre-industrial CO ₂ concentration
T_0	K	pre-industrial temperature
Q_0	Mbook	initial active knowledge amount
f_0		pre-industrial share of fossil fuels
u_{in}		initial value of relative CO ₂ excess
<i>Dimensionless variables</i> (see (28) for definitions)		
x		normalized time
y		normalized active knowledge amount
z		normalized population
u		relative CO ₂ excess
<i>Scale factors</i> (see (29))		
N_s	billion	population scale
Q_s	Mbook	knowledge amount scale
Q_w	Mbook	remainder term in equation (42)
τ_s	year	time scale of population change
τ_c	year	time scale of CO ₂ concentration change (17)
<i>Dimensionless parameters</i> (see (34))		
α		inhibition parameter
β		temperature sensitivity
γ		dissipation parameter
δ		CO ₂ emissions parameter
ε		population/CO ₂ timescales ratio
η		fuel consumption parameter
ν		coefficient of knowledge loss
<i>Standard deviations in the fitting procedure</i>		
s_N	billion	s.d. of population
s_f		s.d. of the share of fossil fuels
s_u		s.d. of CO ₂ excess
s_Q	Mbook	s.d. of active knowledge amount

5. Model calibration

The normalized model (30) – (32) includes dimensionless parameters $\alpha, \beta, \gamma, \eta, \delta, \varepsilon, \nu$ (parameters z_0, g , and d are fixed). To convert them to dimensional ones, we also need to find scale factors τ_s, Q_s , and N_s . All these parameters are determined by fitting to empirical data, which include the following time series:

- carbon dioxide concentration C ,
- world population N ,
- share of fossil fuels f in total energy consumption, and
- book stock Q_{LC} in the Library of Congress as a repository of knowledge.

The calibration procedure is to find parameter values that minimize the deviation of the model from the data. Parameters ν and β are regarded as control ones. Their physical meaning is as follows: ν is the coefficient of knowledge loss, and β is the sensitivity of population to temperature rise. The control parameters are not involved in the calibration and can freely vary in certain ranges. The other parameters must satisfy the minimum deviation condition, which turns them into functions of ν and β . To reduce uncertainty, the calibration is divided into four steps.

5.1. Step 1: Population

The subset $P = \{\alpha, \gamma, N_s, \tau_s\}$ of model parameters is considered. The minimum variance is determined as

$$V_N(\nu, \beta) = \min_P \sum_{i=1}^n \omega_i \left(N(t_i; P, \nu, \beta) - N_{\text{aprx}}(t_i) \right)^2, \quad (35)$$

where

$$N(t) = N_s z(x), \quad x = \frac{t}{\tau_s}, \quad \omega_i = \frac{t_i - t_{i-1}}{t_n - t_0}, \quad (36)$$

ω_i is the weight factor, n is the number of points. Function $z(x)$ is found by solving a pair of equations (30) and (31) with initial conditions

$$y(0) = 0, \quad z(0) = z_0 = 0.055. \quad (37)$$

Function $u(x)$ presented in (31) is calculated here as $u = C_{\text{aprx}}/C_0 - 1$ (instead of (32)), where C_{aprx} is defined by the two regressions shown in Fig. 2. In equation (35), $N_{\text{aprx}}(t)$ is the population time series approximation indicated in Fig. 6. At the output of this step, we obtain the optimal parameters' values: $P = P_{\text{opt}}(\nu, \beta)$.

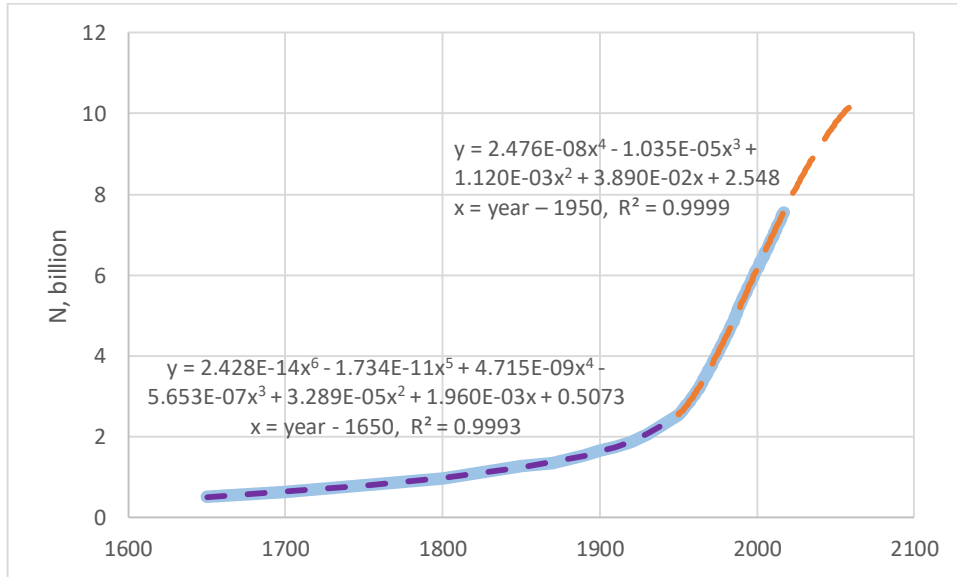


Fig. 6. Population time series (solid curve) and trends in the intervals of 1650 – 1950 and 1950 – 2017 (dashed curves). Data source: [US Census Bureau, 2018](#).

5.2. Step 2: Share of fossil fuels

Now we consider the subset of parameters $P = \{f_0, \eta\}$ belonging to the function

$f(x) = f_0 e^{-\eta y^2(x)}$ (see Section 3.4). The minimum variance is

$$V_f(\nu, \beta) = \min_P \sum_{i=1}^n \omega_i \left(f(x_i; P, \nu, \beta) - f_{\text{aprx}}(t_i) \right)^2, \quad (38)$$

where $x_i = t_i / \tau_s$; $f_{\text{aprx}}(t)$ is the data approximation specified in Fig. 7. Function $y(x)$ present in the expression for $f(x)$ is found from equation (30), in which z is calculated as $z(x) = N_{\text{aprx}}(t) / N_s$ instead of equation (31). As before, the optimal parameters' values depend on v and β .

Approximation in Fig. 7 represents the envelope, which is built according to the data for 1960–1973, 2012–2016, and 2040 (the last point is BP projection for 2040). Data for 1974 – 2011 correspond to the growth of nuclear energetics (Fig. 8), which by 2011 had ceased because of safety problems. These data are not used for calibration since they describe a temporary deviation from the trend; this deviation is associated with unjustified expectations regarding nuclear power. Over time, the share of fossil fuels returned to the level provided by relatively safe energy production technologies. Along with the BP projection until 2040, our projection for 2050, obtained by extrapolating the trends of various energy sources, is presented in Fig. 7; the trends are shown in Fig. 8 and described in Table 2. It can be seen that our projection is consistent with the BP one.

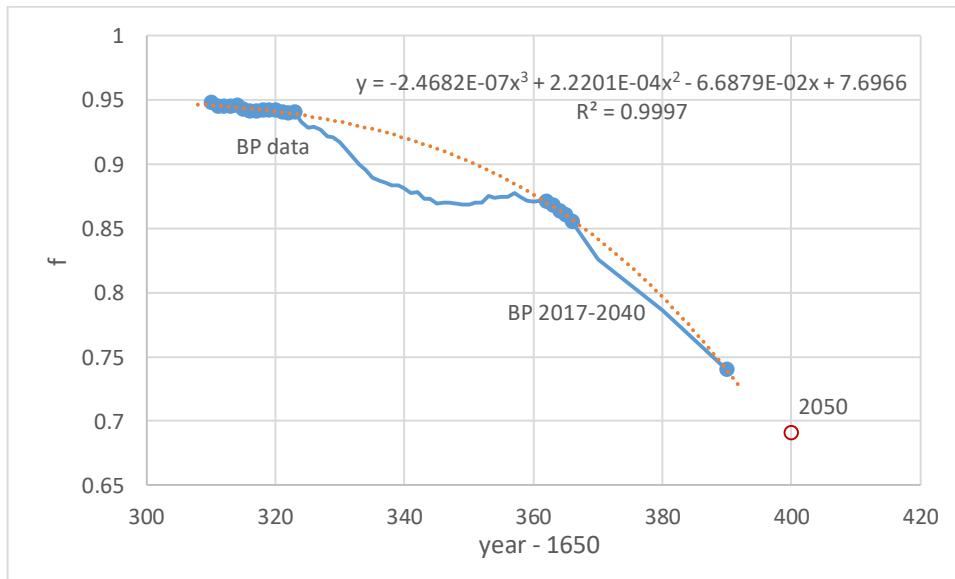


Fig. 7. The share of fossil fuels in total energy consumption and its trend (dotted curve). Filled circles: data used to find the regression. Empty circle: our projection for 2050. Data source: [BP, 2018](#).

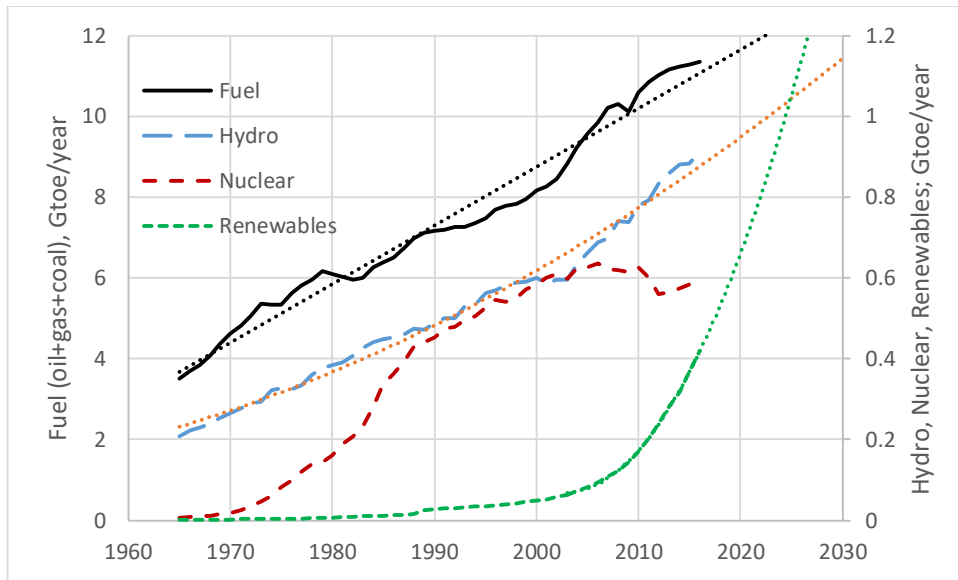


Fig. 8. Time series of various sources of energy consumption and their trends (dotted curves). The trends are described in Table 2. Data source: [BP, 2018](#).

Table 2. World energy consumption (Gtoe/year) in 2016 and projection for 2050

Energy sources	2016**	% total	Trends (x=year, y=energy consumption)	2050	% total
Fuel (oil+gas+coal)	11.35	85.5	$y = 0.1448x - 280.89$, $R^2 = 0.9721$	15.97	69.1
Hydro	0.91	6.9	$y = 9.942E-05x^2 - 3.832E-01x + 3.693E+02$, $R^2 = 0.9863$	1.51	6.6
Nuclear	0.59	4.4	Estimate	1.00	4.3
Renewables*	0.42	3.2	$y = 1.982E-03x^2 - 7.937E+00x + 7.948E+03$, $R^2 = 0.9995$	4.62	20.0
Total	13.27	100		23.10	100

*Gross generation from renewable sources includes wind, geothermal, solar, biomass and waste.

**Data source: [BP, 2018](#).

5.3. Step 3: CO_2 concentration

In this step, we consider the subset of parameters $P = \{\varepsilon, u_{in}\}$. Calibration is carried out in the interval 1800 – present, because earlier data are rare and unreliable. Since the initial moment has shifted from 1650 to 1800, it is necessary to change the CO_2 excess initial value $u(0)$. In (32) there was $u(0) = 0$, and now it should be $u(0) = u_{in}$; the term u_{in} must be added to equation (32) in front of the integral. The minimum variance is

$$V_C(v, \beta) = \min_P \sum_{i=1}^n \omega_i \left(C(t_i; P, v, \beta) - C_{\text{aprx}}(t_i) \right)^2, \quad (39)$$

where $C(t) = C_0(1 + u(x))$, $x = t/\tau_s$; $C_{\text{aprx}}(t)$ is calculated using the regression shown in Fig. 1. Function $u(x)$ is found by solving a pair of equations (30) and (32). In (30), variable z is calculated as $z(x) = N_{\text{aprx}}(t)/N_s$, where $x = t/\tau_s$; $N_{\text{aprx}}(t)$ is shown in Fig. 6. Equation (30) is solved in the interval 1650 – present with the initial condition $y(0) = 0$ corresponding to 1650.

The aforementioned shift of the initial moment from 1650 to 1800 in the calculation of C while all other model equations are calculated starting from 1650, leads to the following change: parameter τ_c participating in the definition of $\varepsilon = t_s/\tau_c$ takes on a different value than that specified in (17). The new value of τ_c must be of the same order as the temporal shift ($\sim 10^2$ years). However, the exponent g in the power-law (17) retains its value, leaving the asymptotic behavior unchanged.

5.4. Step 4: Knowledge

Now we can calculate dynamics of the variables x, y, z using equations (30) – (32). The relationship between y and Q is

$$Q(t) = Q_s y(x), \quad x = \frac{t}{\tau_s}. \quad (40)$$

Dynamics of knowledge accumulation is reflected in the development of the largest repository of knowledge – the Library of Congress (LC) (Fig. 9). To calibrate the model, we used data on the size of the book stock (number of volumes) for 1898 – 1982. During this period, the report form did not change. The change happened after 1982, when an increasing part of the Library's budget begins to be spent on computer carriers, so the method of assessing knowledge growth only by books becomes inadequate since it underestimates the actual increase in knowledge.

We assume a linear relationship between world knowledge amount Q and the LC book stock Q_{LC} :

$$Q(t) = \kappa Q_{\text{LC}}(t) + Q_w, \quad (41)$$

where κ is a coefficient converting the number of books in LC into the total number of books in the world, and Q_w is a remainder term. The LC book stock records are approximated by polynomial regression, shown in Fig. 9. Since there are no data to calculate the conversion coefficient κ in (41), we put $\kappa = 1$, thereby measuring the amount of knowledge in the “LC book equivalent” units (further for short we write simply “book”). In these units we have

$$Q(t) = Q_{LC}(t) + Q_w. \quad (42)$$

The minimum variance is

$$V_Q(v, \beta) = \min_{Q_s, Q_w} \sum_{i=1}^n \omega_i (Q_s y(x_i; v, \beta) - Q_{LC}(t_i) - Q_w)^2. \quad (43)$$

The optimum of Q_s and Q_w is a function of v and β .

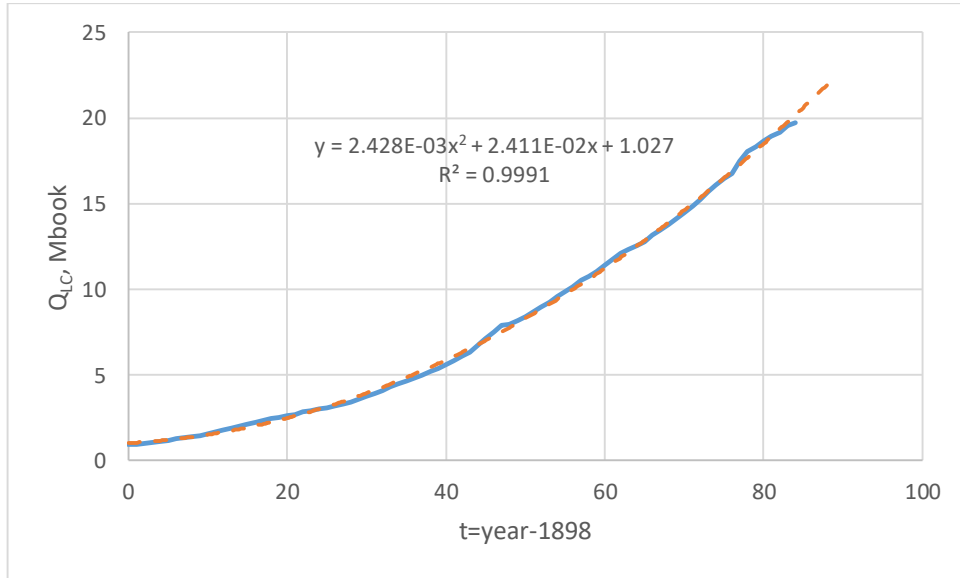


Fig. 9. Book stock of the Library of Congress for 1898 – 1982 (solid curve: data; dashed curve: trend). Only books (volumes, excluding pamphlets) are counted. The three-year gap between 1942 and 1944 was filled by linear interpolation. Data source: [Library of Congress, 2017](#).

6. Results

The four-step procedure of minimizing deviations determines the dimensionless parameters α , γ , δ , ε , η , f_0 , scale factors N_s , τ_s , Q_s , and parameter Q_w , each as a function of v and β .

The calculations according to equations (30) – (32) were carried out using the following constant parameters collected from the previous sections:

$$\begin{aligned} \vartheta &= 3.3917 \text{ K}, \quad C_0 = 276.41 \text{ ppm}, \quad T_0 = 286.66 \text{ K}, \\ p &= 0.2194 \text{ ppm/Gtoe}, \quad K = 0.6620 \text{ Gtoe/year/billion}^{1.5}, \end{aligned} \quad (44)$$

with initial conditions $y_0 = 0$, $z_0 = 0.055$ for $t = 0$ (year 1650).

The dynamics were calculated for the following variables: population N , relative CO₂ excess $u = C/C_0 - 1$, temperature anomaly ΔT , and active knowledge amount Q . About 90 different scenarios were calculated to a depth of several thousand years, and if necessary (e.g., to determine the critical curve; see below) up to 1 million years.

6.1. The critical curve

All scenarios end with either a finite steady state or the collapse of civilization with its complete disappearance. The critical curve $\beta(v)$ separating these two final states is shown in Fig. 10. Its intersections with the axes are $\beta(0) = \beta^* = 3.415$ and $\beta(v^*) = 0$, where $v^* = 0.0467$ is the endpoint beyond which only such a civilization can exist that is insensitive to temperature rise.

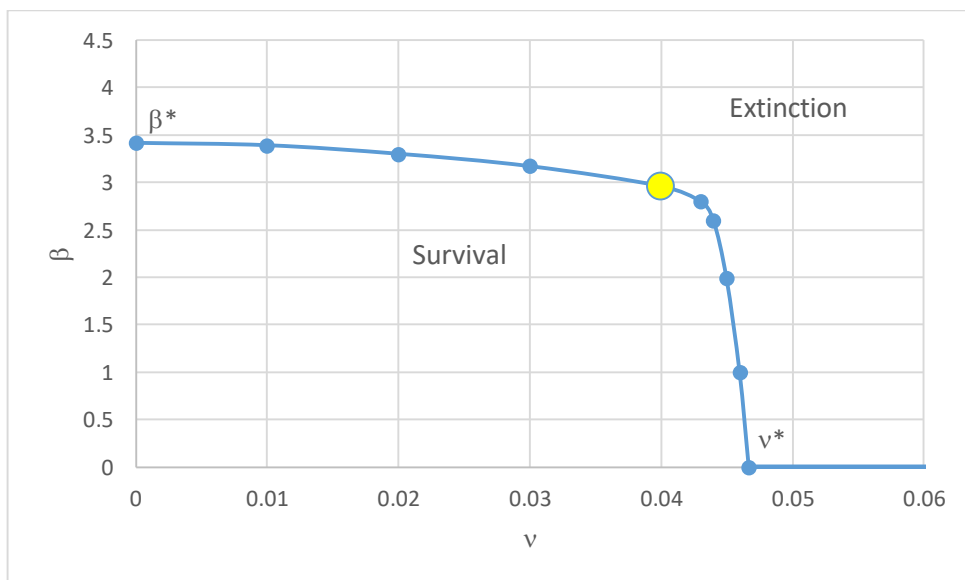


Fig. 10. The critical curve $\beta(v)$, separating the areas where civilization survives or perishes. The highlighted point shows the most probable place of civilization (see Section 7).

In the case of zero loss of knowledge ($\nu = 0$), the existence of civilization is possible in the widest range of β : from absolute temperature insensitivity $\beta = 0$ to high sensitivity $\beta = \beta^*$. With increasing knowledge loss, the admissible sensitivity range gradually narrows, and after passing $\nu = 0.043$, the sensitivity on the critical curve rapidly decreases and vanishes at $\nu = \nu^*$.

Figure 11 shows the lifetime of civilization in the supercritical area. Four cross-sections of the critical curve corresponding to the loss coefficient $\nu = 0, 0.04, 0.05$ and 0.1 are presented. At high sensitivity, lifetime is short: for $\beta = 4$, extinction occurs between 2300 and 2400. As sensitivity decreases, lifetime increases, tending to infinity when approaching the critical curve. For example, collapse occurs after 280 thousand years for $\nu = 0.05$ and $\beta = 2.5$, and after 38 thousand years for $\nu = 0.1$ and $\beta = 1$ (both lifetimes are far beyond the graph). Smaller β values correspond to lifetimes in millions of years. In this case, we can regard civilization as metastable since it is in the supercritical area and is doomed to extinction, albeit in a very distant future (however, there is hope that for such a long time, favorable changes can occur in civilization or the environment, but this matter is beyond the scope of the model).

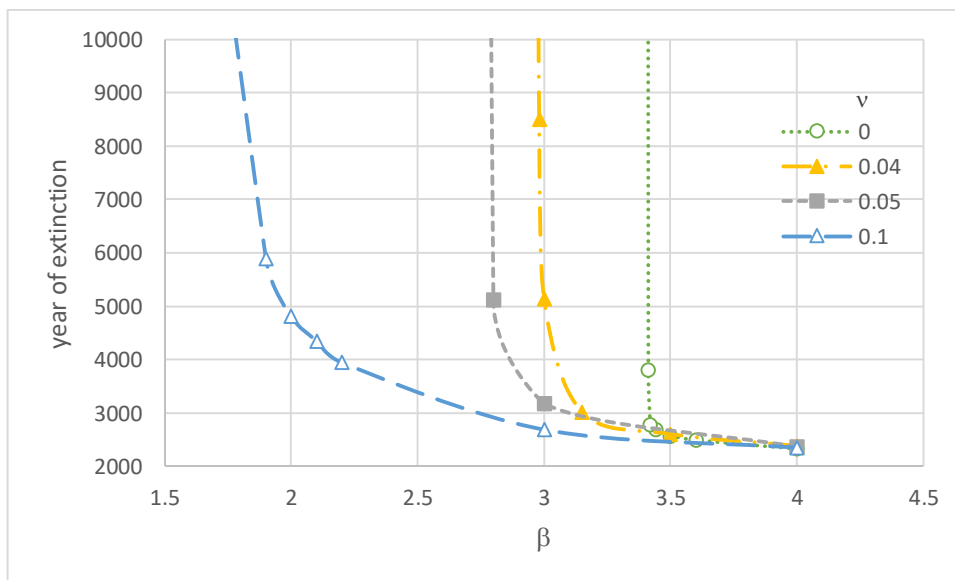


Fig. 11. The year of extinction, defined as the year when the population falls below 0.1 billion.

6.2. Development scenarios

Let us consider several calculated scenarios of the transition through the critical curve in three cross-sections $\nu = 0.01, 0.04$, and 0.1 (Figs. 12 – 14). Each scenario is characterized by two parameters: knowledge loss coefficient ν and sensitivity of population to temperature rise β . Information on scenarios with different values of β in these cross-sections is presented in Table 3.

6.2.1. Low knowledge loss

Scenarios with a low loss coefficient $\nu = 0.01$ are presented in Fig. 12. The left panels show good agreement with empirical data for all scenarios, regardless of temperature sensitivity. The scenarios diverge over time. This is especially noticeable concerning the population, which in different scenarios varies significantly by the mid-century. In a more distant future, the scenarios radically diverge as shown in the right panels which demonstrate dynamics up to 5600.

In the case of absolute insensitivity to temperature rise ($\beta = 0$), the population by the end-century almost reaches a plateau of 10.1 billion people. A little later, CO_2 excess and temperature reach their maximums $u = 1.34$ and $T = 16.3^\circ\text{C}$; the latter is 1.4°C higher than the temperature of 2017 (14.9°C). At the same time, active knowledge amount is growing rapidly.

With increasing temperature sensitivity, population dynamics become more complex. For $\beta = 2.8$, the population reaches a maximum of 9.3 billion in 2058, then over two centuries, population drops to a minimum of 8.1 billion in 2251. After that, growth resumes, asymptotically tending to a plateau of 10.3 billion.

A similar situation holds for the pre-critical sensitivity $\beta = 3.39$. The population maximum of 9 billion falls in 2050, and the minimum becomes deeper, 4.8 billion in 2512. Then there is a slow growth to a plateau of 10.4 billion.

A barely noticeable increase in sensitivity β from 3.39 to 3.40 leads to catastrophic consequences: after a maximum of 9 billion in 2050, there is a decline in the population, which until 2300 practically coincides with the previous non-catastrophic scenario. However, further the decline does not stop, and by 2940 the population falls below the level of 0.1 billion (which we conditionally accept as the moment of the disappearance of civilization).

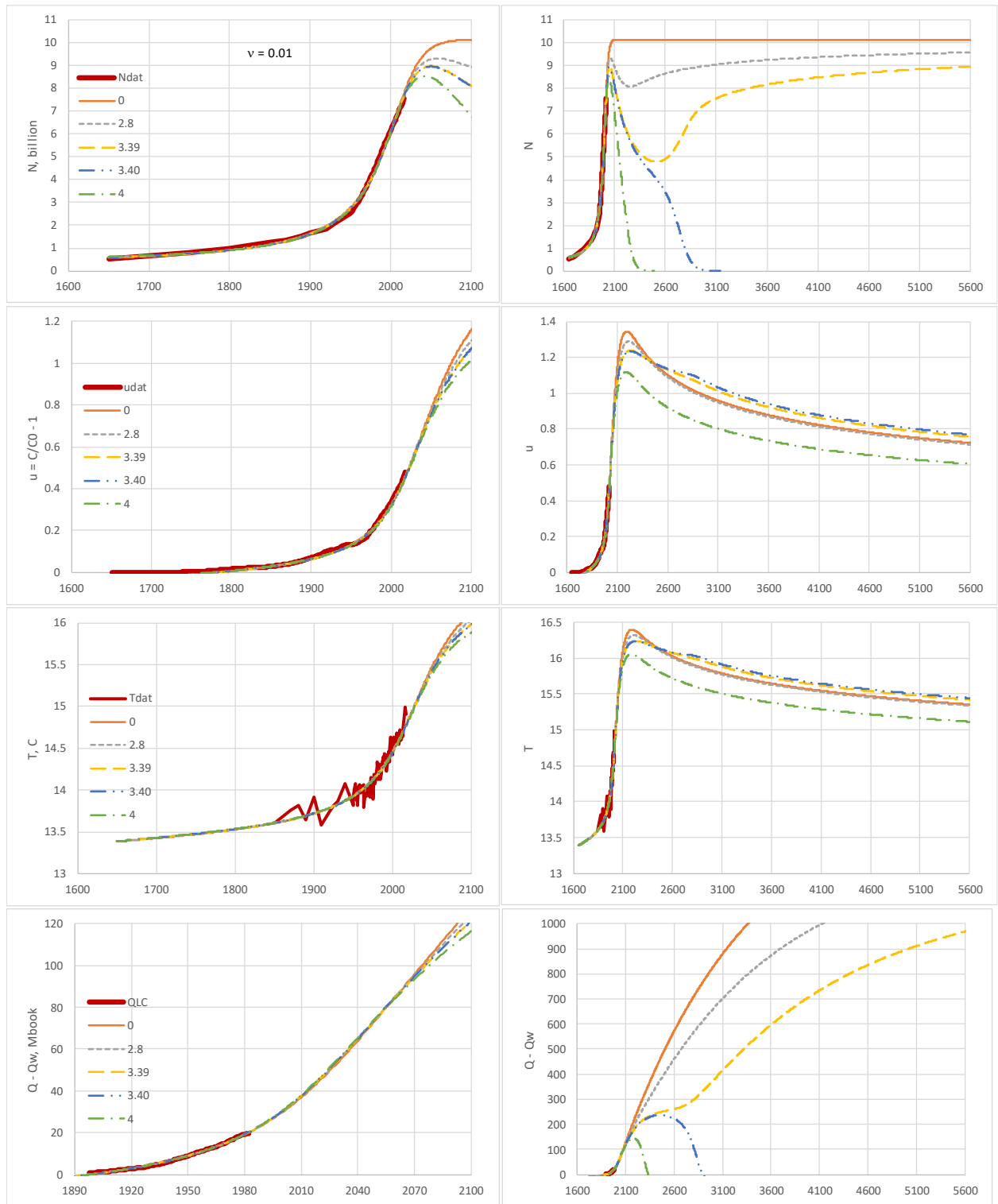


Fig. 12. Dynamics of population, CO₂ excess, temperature, and active knowledge amount: scenarios with loss coefficient $\nu = 0.01$. Legend: data and temperature sensitivity β values. Left panels: projections until 2100 and comparison with historical data. Right panels: projections until 5600.

Even more rapid disappearance of civilization occurs for high sensitivity $\beta = 4$: a maximum of 8.6 billion is reached in 2042, and the collapse occurs as early as 2348.

In the above scenarios, the temperature reaches a maximum of $16 - 16.5^\circ\text{C}$ around 2200, and then it slowly decreases due to a decrease in CO_2 excess over tens of thousands of years (tails relax even longer, over hundreds of thousands of years).

The amount of active knowledge (more precisely, the difference $Q - Q_w$) in subcritical scenarios ($\beta = 0, 2.8$, and 3.39) increases reaching a high plateau (~ 1500 Mbook, Table 3), whereas in supercritical scenarios ($\beta = 3.4$ and 4), active knowledge goes through a maximum (an order of magnitude lower than the mentioned plateau), and then disappears simultaneously with the collapse of civilization.

6.2.2. Medium knowledge loss

As the loss coefficient increases, scenarios change. The situation for $v = 0.04$ is shown in Fig. 13. The left panels show good agreement with the data. The discrepancy between different scenarios become noticeable since the mid-century. The transition through the critical curve occurs for β between 2.96 and 2.97. The right panels show a dramatic change in scenarios when crossing the critical curve. In the subcritical area, after passing through a maximum and a minimum, the population increases reaching a plateau (slightly above 10 billion, scenarios $\beta = 2.7, 2.9, 2.96$). In the supercritical area (scenarios $\beta > 2.96$), population eventually collapses; its lifetime is very long near the critical curve and decreases with distance from it (with increasing β) as shown in Fig. 11 and Table 3. The scenario $\beta = 2.97$ is not shown in Fig. 13, since in the time interval depicted it is practically indistinguishable from the scenario $\beta = 2.96$, but deviates strongly from the latter at a more distant time, experiencing a collapse after almost 20 thousand years.

The temperature in the subcritical area ($\beta \leq 2.96$) reaches a maximum (about 16.3°C), and then slowly decreases due to a decrease in CO_2 excess. In the supercritical area (scenario $\beta > 2.96$), the temperature behavior depends on the proximity to the critical curve. In its vicinity, temperature increases (possibly after a certain decrease, as for $\beta = 2.97$ and 3) and eventually becomes intolerable for the population, which begins to decline in size rapidly, leading to a decrease in CO_2 emissions and temperature. The second temperature maximum for $\beta = 2.97$

(equal to 17.1°C) is not visible in Fig. 13, since it falls on the year 20181, after which civilization quickly collapses (in 20292). For $\beta = 3$, the second temperature maximum (also about 17.1°C) is much closer, namely in 5007, and the collapse year is 5127. With very high sensitivity (scenario $\beta = 4$), the population drops so quickly that distant temperature peaks disappear, and the temperature begins to decline immediately after passing the first maximum of 16.2°C in 2249, and after 129 years a collapse occurs. Note that CO_2 excess has the same dynamics.

Active knowledge in the subcritical area grows, reaching a plateau (568, 495, and 463 Mbook for the first three scenarios in Fig. 13), which is significantly lower than that in the corresponding group of scenarios for $\nu = 0.01$. In the supercritical area, active knowledge is nullified along with the disappearance of civilization.

6.2.3. High knowledge loss

With a high value of the loss coefficient $\nu = 0.1$, the only scenario that preserves civilization corresponds to absolute insensitivity to temperature rise, $\beta = 0$. Any finite sensitivity leads to the collapse of civilization over time. This situation is illustrated in Fig. 14, which presents several scenarios with different β values. For $\beta > 0$ and a high loss of knowledge, civilization is not able to create environment-friendly life-support technologies that would ensure sustainable development. Under increasing heat stress, the population is declining. The comparative population and CO_2 dynamics (right panels N and u in Fig. 14) show that shortly after passing the CO_2 maximum (which coincides with the temperature one), civilization collapses. In parallel with population decline, the active knowledge amount is also decreasing. Details are presented in Table 3.

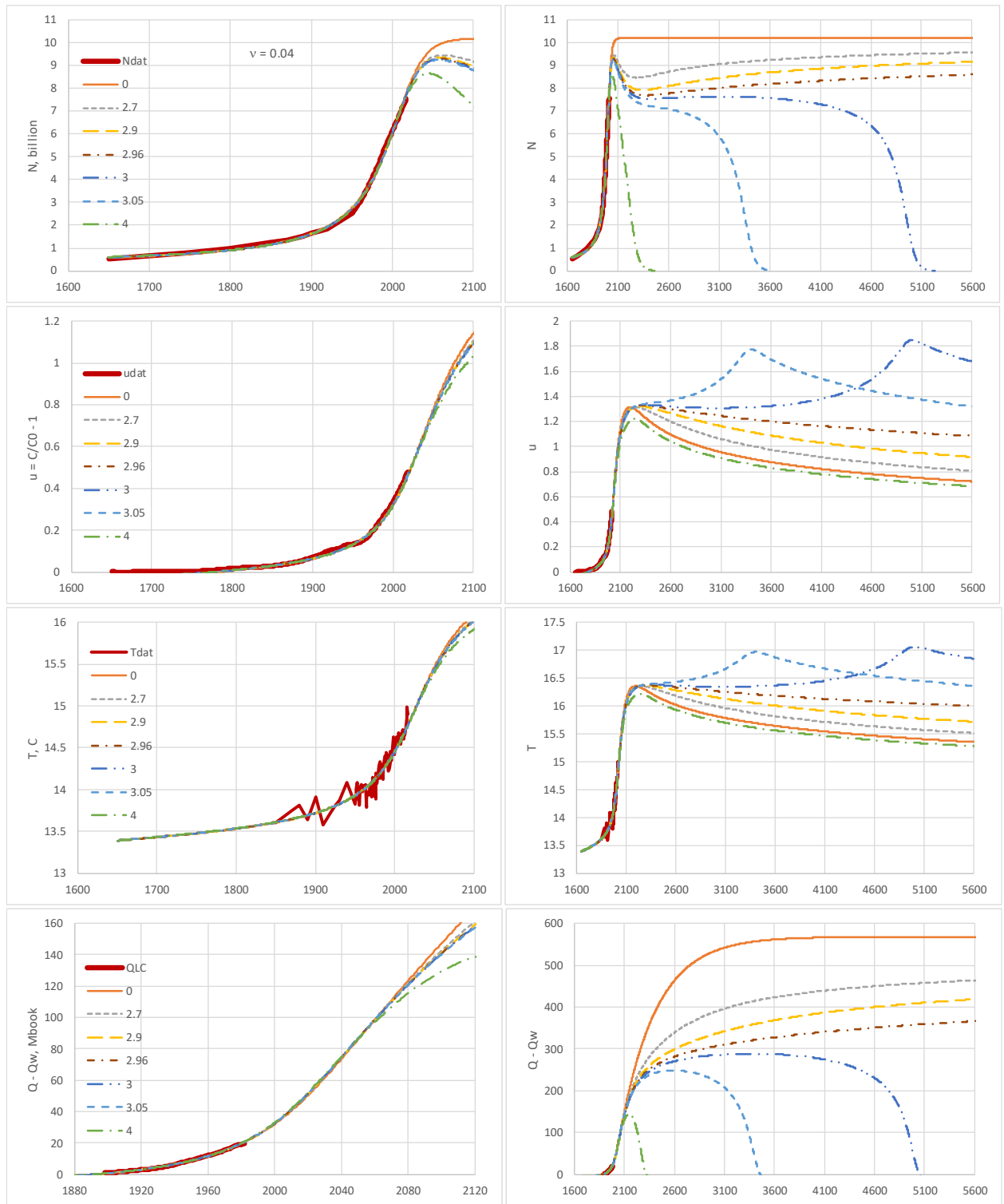


Fig. 13. Scenarios with loss coefficient $v = 0.04$.

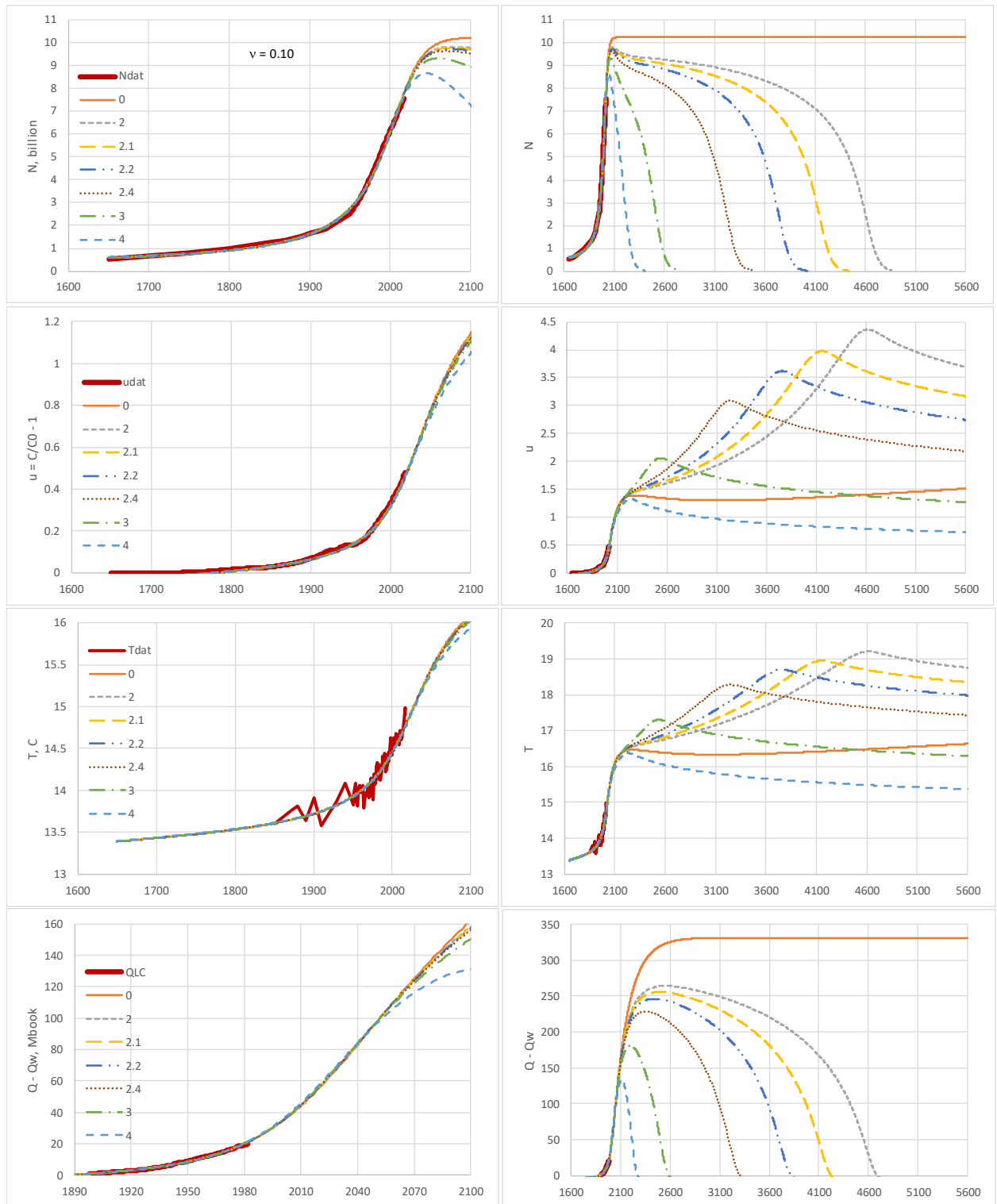


Fig. 14. Scenarios with loss coefficient $\nu = 0.1$.

Table 3. Characteristics of selected scenarios*

v	β	α	γ	N_s	τ_s	Q_s	Q_w	f_0	η	τ_c	u_{in}	δ	ε	N maximum**		N minimum		N plateau	Extinction	T maximum**		(Q-Q _w) maximum‡	
				billion	year	Mbook	Mbook			year				year AD	billion	year AD	billion	billion	year AD	year AD	°C	year AD	Mbook
0.01	4	1.08	0.0345	11.2	11.5	16.0	13.19	0.977	0.0105	108	-0.0355	0.220	0.106	2042	8.6			0	2348	2187	16.1	2182	145
	3.40	1.22	0.0319	10.9	12.1	16.0	13.44	0.978	0.0109	107	-0.0354	0.225	0.113	2050	9.0			0	2940	2228	16.2	2457	237
	3.39	1.20	0.0317	10.9	12.2	16.1	13.47	0.978	0.0110	107	-0.0356	0.226	0.113	2050	9.0	2512	4.8	10.4		2228	16.2		1447
	2.8	1.26	0.0294	10.7	12.7	16.2	13.69	0.979	0.0114	107	-0.0356	0.231	0.119	2058	9.3	2251	8.1	10.3		2212	16.3		1484
	0	1.26	0.0242	10.4	14.0	16.7	14.14	0.981	0.0125	106	-0.0356	0.242	0.132					10.1		2191	16.4		1573
0.04	4	1.44	0.0316	11.1	12.6	24.1	7.55	0.959	0.0211	114	-0.0343	0.234	0.110	2044	8.7			0	2378	2249	16.2	2149	144
	3.75	1.56	0.0317	11.1	12.5	23.9	7.53	0.959	0.0209	114	-0.0344	0.233	0.109	2047	8.8			0	2427	2293	16.3	2167	155
	3.6	1.59	0.0311	11.0	12.7	23.9	7.59	0.959	0.0211	114	-0.0344	0.234	0.111	2050	8.9			0	2484	2346	16.4	2187	165
	3.45	1.61	0.0305	11.0	12.8	23.9	7.65	0.959	0.0212	114	-0.0344	0.235	0.112	2051	9.0			0	2566	2426	16.5	2215	178
	3.3	1.62	0.0298	10.9	13.0	23.9	7.72	0.959	0.0214	114	-0.0344	0.237	0.114	2054	9.1			0	2707	2567	16.6	2262	195
	3.15	1.64	0.0292	10.9	13.1	23.9	7.77	0.959	0.0215	114	-0.0344	0.238	0.115	2056	9.2			0	2990	2854	16.8	2359	219
	3.05	1.65	0.0288	10.9	13.2	23.9	7.81	0.960	0.0216	114	-0.0345	0.239	0.116	2057	9.3			0	3535	3406	17.0	2594	248
	3	1.64	0.0285	10.8	13.3	23.9	7.84	0.960	0.0217	113	-0.0344	0.239	0.117	2058	9.3	2427	7.5	0	5127	2354	16.4	3376	288
	2.97	1.65	0.0284	10.8	13.3	23.9	7.85	0.960	0.0217	114	-0.0345	0.239	0.117	2058	9.3	2391	7.7	0	20292	2341	16.4	11174	363
	2.96	1.65	0.0284	10.8	13.3	23.9	7.85	0.960	0.0217	114	-0.0345	0.239	0.117	2058	9.3	2381	7.7	10.2		2320	16.4		516
	2.9	1.65	0.0281	10.8	13.4	23.9	7.88	0.960	0.0218	114	-0.0345	0.240	0.118	2060	9.3	2339	7.9	10.3		2289	16.4		536
	2.7	1.65	0.0273	10.8	13.6	23.9	7.95	0.960	0.0219	114	-0.0345	0.242	0.119	2062	9.5	2288	8.5	10.3		2251	16.4		544
	1.5	1.65	0.0240	10.5	14.4	24.1	8.25	0.961	0.0228	113	-0.0344	0.249	0.128	2086	10.0	2225	9.8	10.2		2203	16.4		550
	0.7	1.64	0.0228	10.5	14.7	24.1	8.36	0.961	0.0230	113	-0.0345	0.251	0.130	2117	10.14	2216	10.13	10.2		2197	16.4		564
	0	1.63	0.0225	10.4	14.8	24.2	8.39	0.961	0.0231	113	-0.0345	0.252	0.131					10.2		2196	16.4		569
0.1	4	2.10	0.0313	11.1	12.8	36.0	4.89	0.951	0.0393	118	-0.0339	0.238	0.108	2046	8.7			0	2349	2235	16.4	2111	133
	3	2.27	0.0273	10.8	13.8	35.5	5.18	0.951	0.0399	118	-0.0340	0.246	0.117	2060	9.3			0	2689	2536	17.3	2197	181
	2.4	2.27	0.0251	10.7	14.3	35.3	5.34	0.952	0.0404	118	-0.0340	0.251	0.122	2070	9.6			0	3421	3242	18.3	2352	229
	2.2	2.28	0.0246	10.7	14.5	35.3	5.37	0.952	0.0405	117	-0.0339	0.252	0.123	2074	9.7			0	3946	3756	18.7	2439	246
	2.1	2.27	0.0243	10.6	14.5	35.3	5.40	0.952	0.0406	117	-0.0339	0.253	0.124	2076	9.8			0	4352	4156	19.0	2496	256
	2	2.28	0.0241	10.6	14.6	35.3	5.41	0.952	0.0406	117	-0.0339	0.253	0.125	2078	9.8			0	4820	4616	19.2	2551	264
	1	2.25	0.0222	10.5	15.0	35.2	5.49	0.952	0.0411	118	-0.0340	0.257	0.128	2100	10.13	2350	10.09	0	38410	2315	16.5	3490	319
	0	2.22	0.0214	10.5	15.2	35.2	5.60	0.952	0.0413	117	-0.0339	0.259	0.130					10.2		2276	16.5		331

*Scenarios ending in extinction are shaded. Empty cells indicate the absence of this category. See Table 1 for the explanation of model parameters.

**The first maximum of the curve is indicated.

‡ If the year is not specified for the $(Q-Q_w)$ maximum, then this is a plateau (formally year = ∞).

6.3. Universality

Population maximums and minimums are functions of the parameters ν and β . However, the calculations reveal universality, which consists in the fact that the ratios $N_{\max}(\nu, \beta)/N_{\text{plat}}(\nu, 0)$ and $N_{\min}(\nu, \beta)/N_{\text{plat}}(\nu, 0)$ are independent of ν , where $N_{\text{plat}}(\nu, 0)$ is the plateau level for $\beta = 0$ when the population is insensitive to temperature rise (the plateau is understood as the limit of N at $t \rightarrow \infty$). The same universality applies to the extremum year (year_{\max} and year_{\min}), which also depends on β but does not depend on ν . The law of universality is illustrated in Fig. 15. Corresponding regressions and determination coefficients are indicated on the panels. An increase in the loss coefficient ν is compensated by an increase in the plateau level: a larger population contributes to a decrease in total losses since N is in the denominator of the corresponding term in equation (23) (or z in the normalized equation (30)). The graphs show that with a decrease in sensitivity in the limit $\beta \rightarrow 0$, the maximum and minimum converge in 2214 and annihilate.

6.4. Population extremums along the critical curve

Population extremums and the years of their appearance change when moving along the critical curve as shown in Fig. 16. For a low loss coefficient ν , the extremums N_{\max} and N_{\min} differ significantly. For $\nu = 0.01$, minimum is present only on the subcritical curve (in Fig. 12 this is the curve $\beta = 3.39$, while the supercritical curve $\beta = 3.40$ close to it does not have minimum). However, with increasing ν (but in the area of $\nu < \nu^*$ where the critical curve exists), minimums appear on both adjacent curves.

For $\nu = 0.04$, the corresponding example is shown in Fig. 13: these are the curves $\beta = 2.96$ and 3. Further, the maximum and minimum gradually approach each other and coincide at the endpoint ν^* , reaching the value $N = 10.2$ billion. For higher values of ν , there are no extremums; only the scenario $\beta = 0$ remains sustainable and reaches a plateau, which rises with ν as shown in Fig. 15. The moments of the appearance of extremums for small ν are quite far from each other (500 years apart for $\nu = 0.01$, see Fig. 16, lower panel). With increasing ν , they gradually get closer and finally coincide ($\text{year}_{\max} = \text{year}_{\min} = 2214$) at the endpoint of the critical curve.

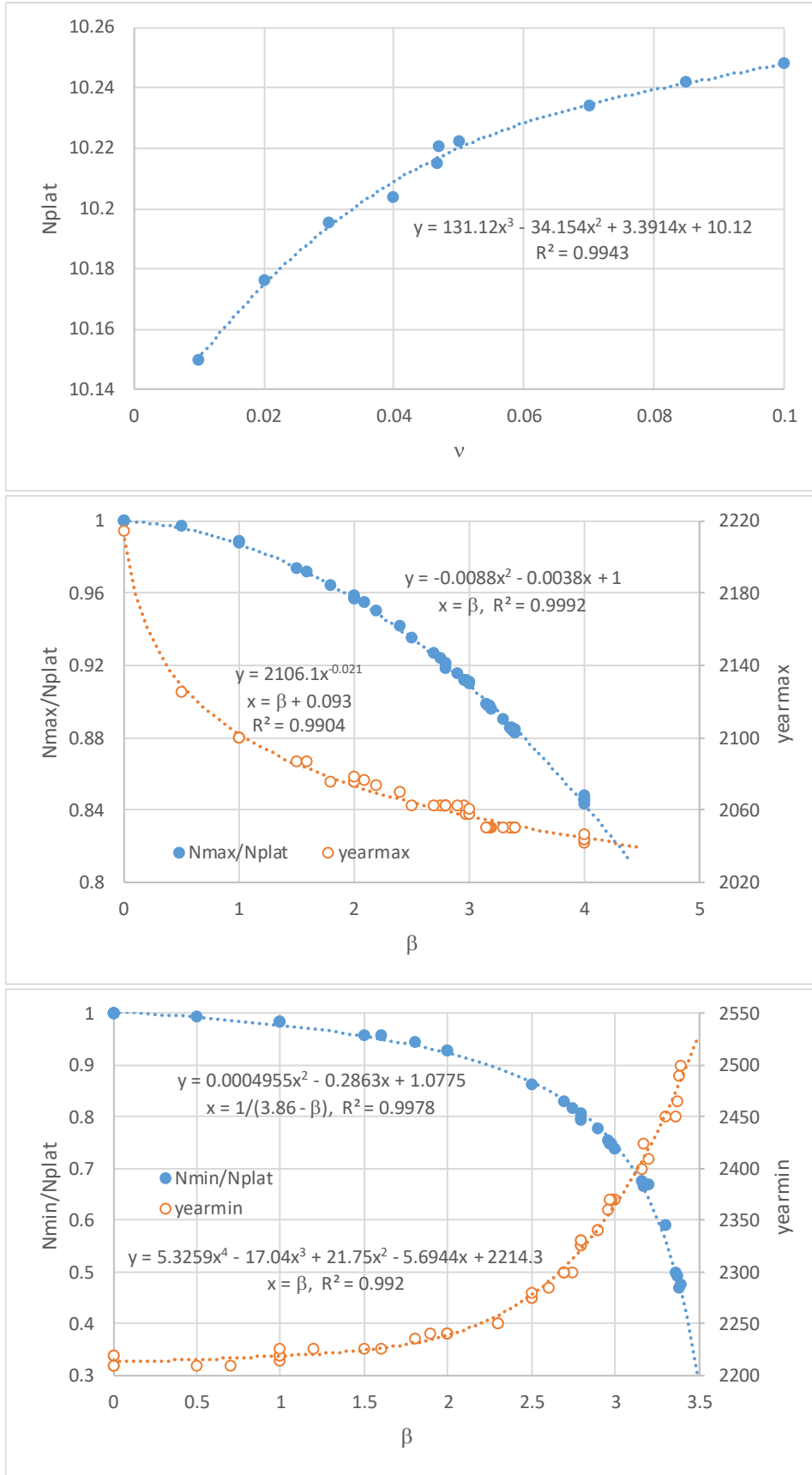


Fig. 15. Stationary population N_{plat} for $\beta = 0$ as a function of v (top panel); population maximum and minimum and years of their appearance as a function of β (middle and lower panels).

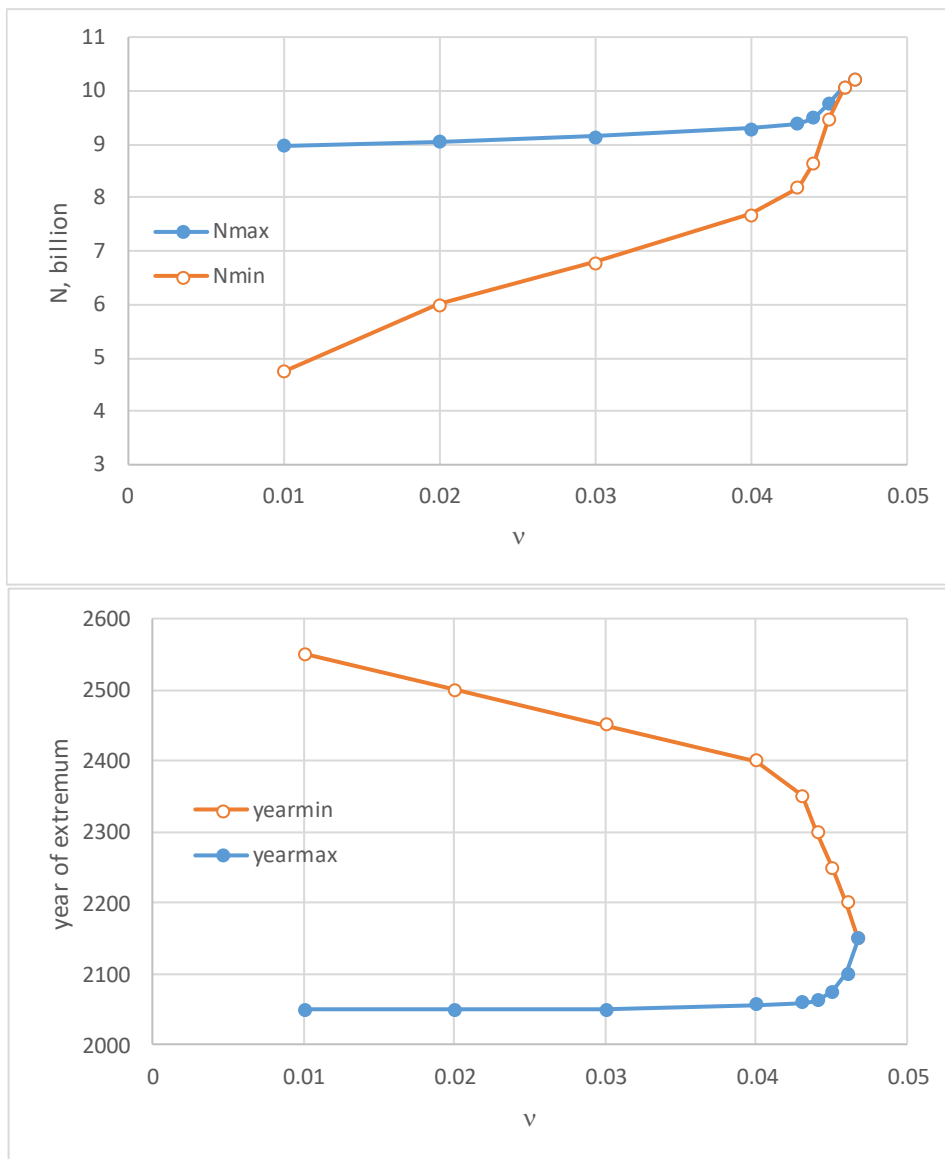


Fig. 16. The first population maximum and minimum and the year of their appearance when moving along the critical curve $\beta(v)$.

6.5. Parameters along the critical curve

The model parameters change when moving along the critical curve as shown in Fig. 17. It is seen that the curves experience a kink at the endpoint v^* of the critical curve. In some cases, the kink is negligible, such as for Q_s , u_{in} and α . The presence of a kink is associated with the loss of stability and the disappearance of civilization with finite temperature sensitivity $\beta > 0$. With a high loss coefficient $v \geq v^*$, survival is only possible with absolute insensitivity to temperature rise ($\beta = 0$).

For population N , the relative error in the data is estimated as 4 – 5% (Burch, 2015). The accuracy of the other data is probably not better. For N , this gives an absolute error of at least 0.3 billion for the current population of 7.7 billion, while calculations deviate from the data to a much lesser extent of about 0.08 billion. Thus, the accuracy of the model calculations is quite acceptable.

6.6. Changing the share of fossil fuels

The results of calculating the share f of fossil fuels in total energy consumption are shown in Fig. 18. The scenario groups for different values of the loss coefficient ν contain subcritical and supercritical scenarios. The first category includes: $\beta = 0$ and 2.8 for $\nu = 0.01$; $\beta = 0$ and 2.7 for $\nu = 0.04$; and only $\beta = 0$ for $\nu = 0.1$. The remaining scenarios fall into the second category. In subcritical scenarios, the share of fossil fuels decreases, asymptotically tending to zero. In supercritical scenarios, the decline in f slows down, and at some point, growth begins, which ultimately leads f to the initial pre-industrial level. This behavior is caused by a loss of knowledge, which forces the remaining population to use readily available fuels, the production of which does not require complex technologies. In the later stages of the process, the loss of knowledge is accompanied by a reduction in the population to complete extinction. The minimum value of f , the moment it appears, and, for comparison, the moment of extinction are listed below for some scenarios:

ν	β	f_{\min}	year _{min}	year _{ext}
0.01	4	0.348	2182	2348
	3.4	0.067	2457	2940
0.04	4	0.417	2149	2378
	3	0.034	3375	5127
0.1	4	0.537	2111	2349
	3	0.315	2197	2689
	2	0.089	2551	4352

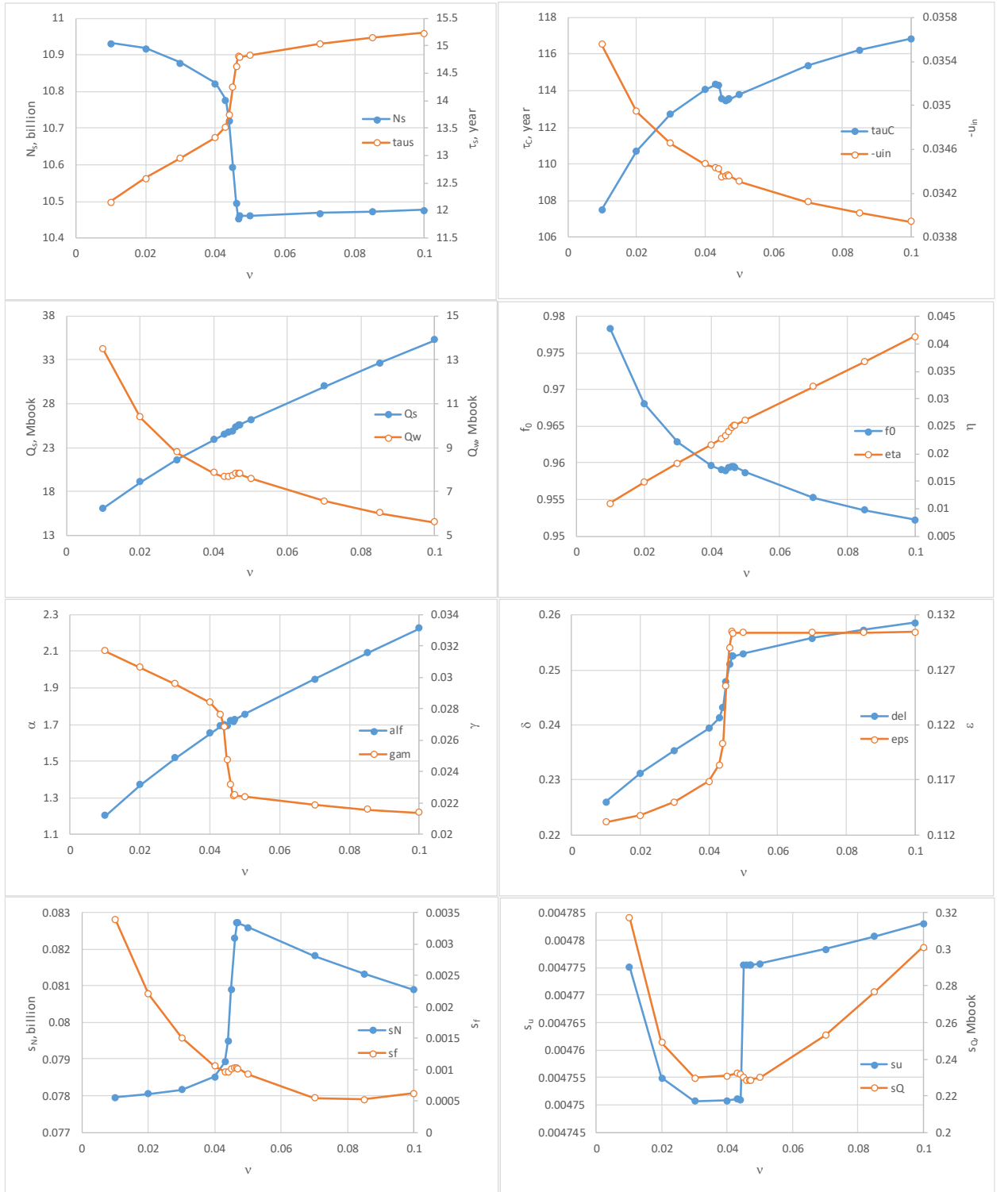


Fig. 17. Model parameters and standard deviations when moving along the critical curve $\beta(\nu)$.

See Table 1 for notations.

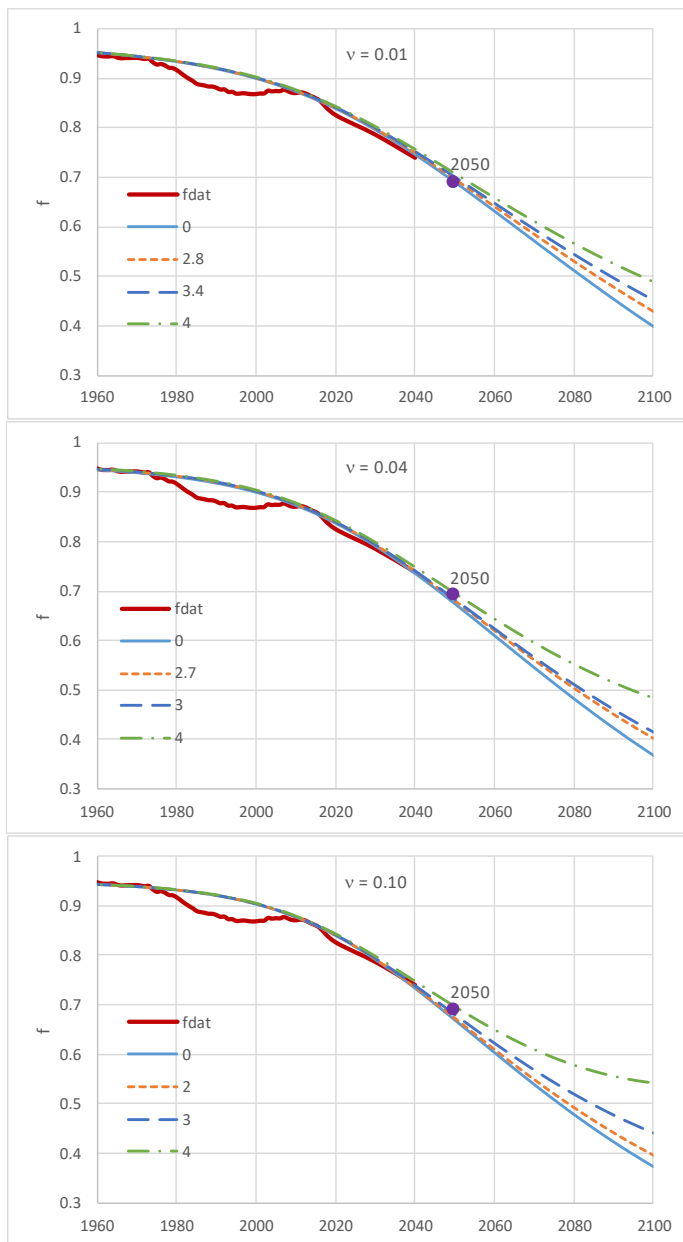


Fig. 18. The share of fossil fuels in total energy consumption for different values of ν and β according to the results of model calculations. For comparison, BP data and BP projection up to 2040, as well as our projection for 2050 (see Section 5.2) are shown. Legend: data and values of β .

7. Discussion

7.1. Physical model parameters

We begin the discussion with the behavior of physical (dimensional) parameters. Given the scale factors (29) and dimensionless parameters (34) calculated earlier for various scenarios, we

can write

$$\sigma = \frac{\vartheta}{\beta}, \quad w = \frac{Q_s}{N_s \tau_s}, \quad v = \frac{1}{b_s} = \frac{Q_s}{\tau_s}, \quad m_s = \frac{1}{h} = \frac{v N_s}{\tau_s},$$

$$\tau_d = \frac{1}{l_s} = \frac{\tau_s}{\gamma}, \quad Q_a = \frac{1}{a} = \frac{Q_s}{\alpha}, \quad Q_c = \frac{1}{\sqrt{c}} = \frac{Q_s}{\sqrt{\eta}}, \quad (45)$$

where σ is the temperature tolerance, w is the specific rate of knowledge production. New parameters that are easier to interpret have also been introduced: v is the scale of knowledge production rate, m_s is the scale of mortality associated with the loss of knowledge, τ_d is the characteristic time of energy dissipation in knowledge production, Q_a is the knowledge amount, upon reaching which the inhibition of knowledge production due to environmental limitations becomes noticeable (regarding inhibition see Sections 2.1 and 2.2), Q_c is the knowledge amount that is needed to reduce the share of fossil fuels in total energy consumption through the transition to alternative (non-hydrocarbon) energy sources. The change in these parameters when moving along the critical curve is shown in Fig. 19.

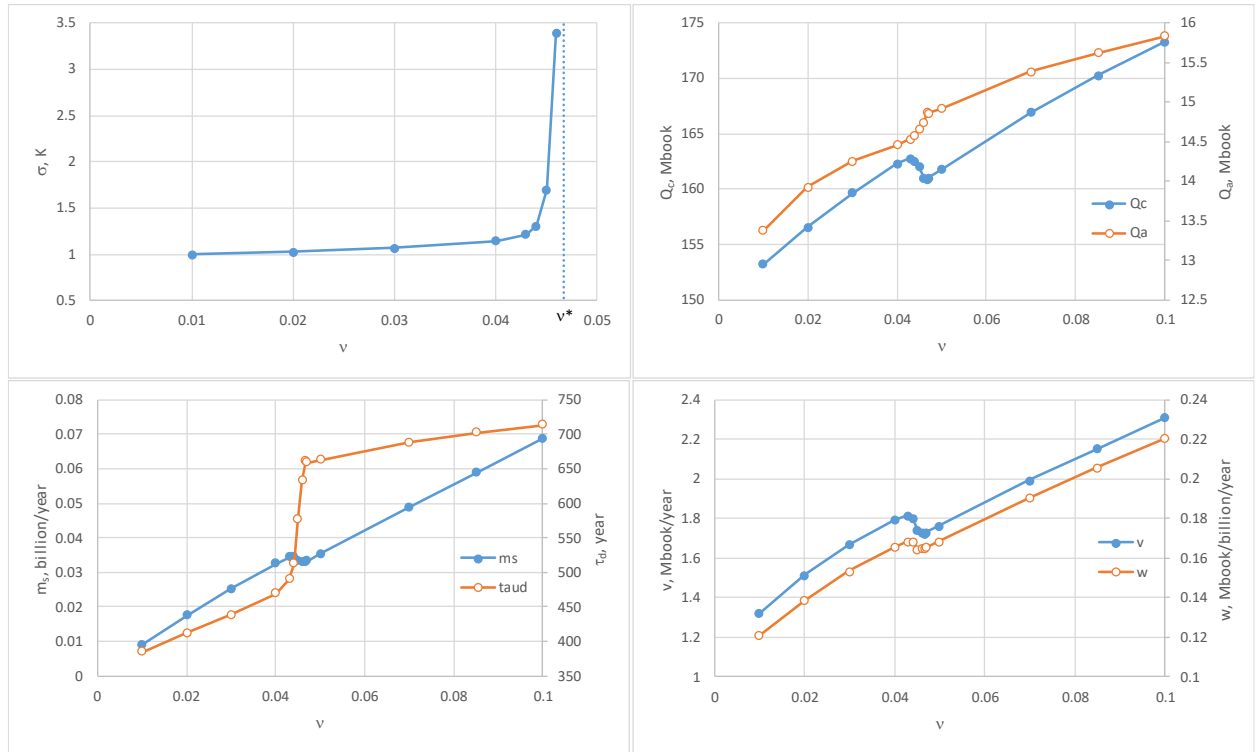


Fig. 19. Physical parameters along the critical curve.

The temperature tolerance σ is close to 1°C far from the endpoint $v^* = 0.0467$, but σ increases unlimitedly as v approaches v^* , where a sustainable civilization must be insensitive to temperature rise.

The scales of knowledge Q_a and Q_c should increase with increasing the loss coefficient v , which is confirmed by calculations (except for the neighborhood of v^*). Moreover, it turns out that Q_c is an order of magnitude larger than Q_a . This can be explained as follows. Civilization in its development and accumulation of knowledge disturbs the environment, and when the negative feedback becomes significant (at $Q \sim Q_a$), civilization is forced to produce a huge amount of knowledge ($Q \sim Q_c$) in order to create new environment-friendly technologies and restore the environment.

With an increase in the loss coefficient v , the mortality rate m_s increases almost linearly from 0.01 to 0.07 billion/year in the considered range of v ; linearity is violated in a small neighborhood of the point v^* , where a kink of the curve is observed.

The characteristic energy dissipation time τ_d varies significantly when passing through the point v^* : from 390 – 470 years for $v \leq 0.04$ to 660 – 720 years for $v > v^*$.

The knowledge production rate v and the specific rate of this process $w = v / N_s$ increase with increasing the loss coefficient (except for the vicinity of the point v^*), and both curves are almost parallel since N_s changes insignificantly, only by 5% (see Fig. 17). According to Fig. 19, the scale v of knowledge production rate varies in the range 1.3 – 2.3 Mbook/year depending on the loss coefficient: larger losses require more production of knowledge when moving along the critical curve (recall that the unit "book" corresponds to the books selected for the book stock of the Library of Congress, see Section 5.4). Based on 1 billion people, 0.12 to 0.22 Mbook/year is produced (see curve w).

7.2. Civilization at the edge of stability

As shown in Sections 5 and 6, two control parameters – coefficient of knowledge loss v and sensitivity of population to temperature rise β – determine all other parameters and thereby control the system dynamics. Let us estimate the most probable values of v and β . To do this, we introduce the total deviation

$$S_{\text{total}} = \frac{1}{4} \sum_X \frac{s_X}{X_{\text{aver}}}, \quad X = N, f, u, Q, \quad (46)$$

where s_X and X_{aver} are the standard deviation and the average value of X :

$N_{\text{aver}} = 4.85$ billion, $f_{\text{aver}} = 0.907$, $u_{\text{aver}} = 0.262$ (each over 1950 – 2017),

$Q_{\text{aver}} = 7.78$ Mbook (over 1898 – 1982);

standard deviations in physical units are shown in Fig. 17 (bottom panels). The total deviation is presented in Fig. 20.

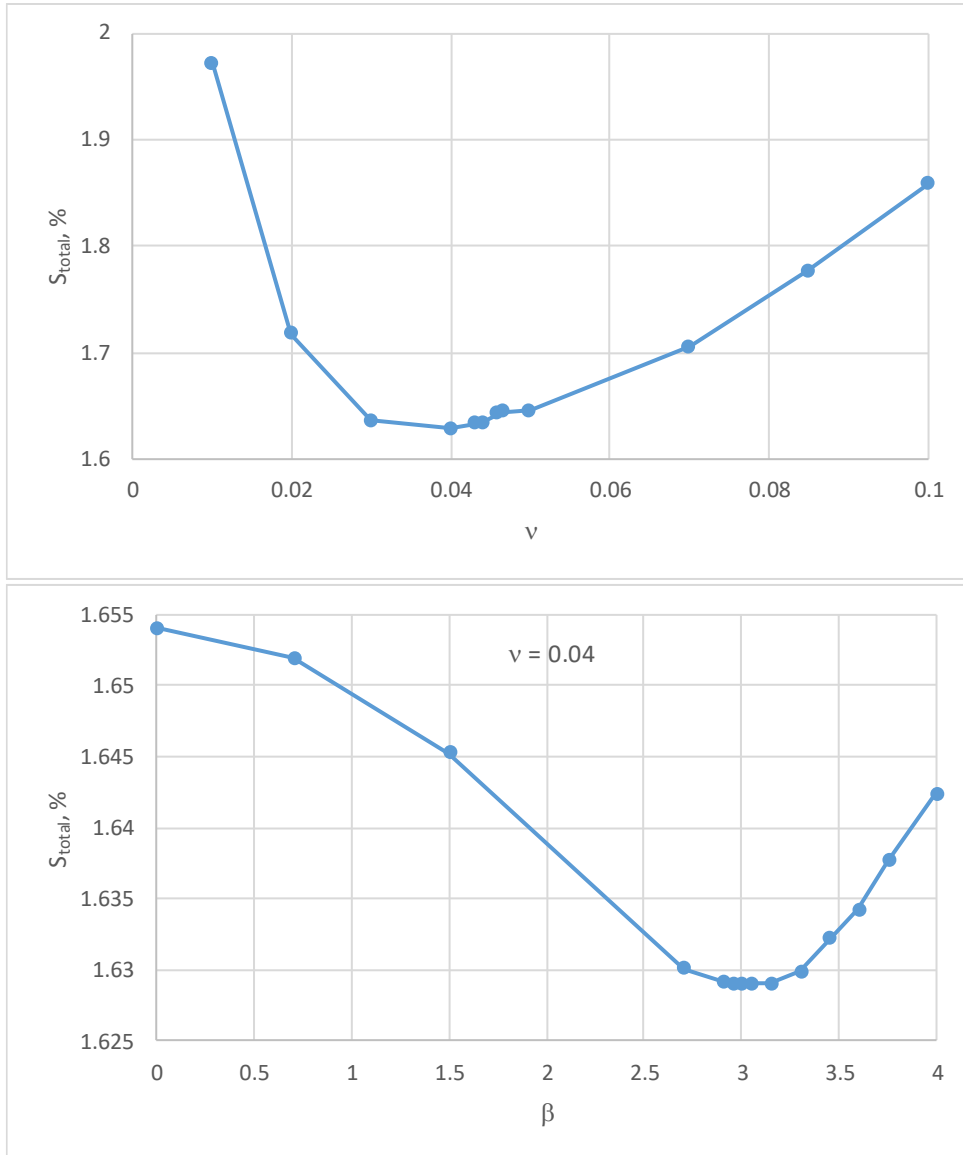


Fig. 20. Total deviation along the critical curve (upper panel) and along the cross-section $v = 0.04$ (lower panel).

S_{total} changes along the critical curve as shown in the upper panel; the minimum is reached at $v_c = 0.04$. The change in S_{total} across the critical curve in the cross-section $v = 0.04$ is shown in the lower panel; the minimum is reached at $\beta_c = 2.96+$ (between 2.96 and 2.97). Thus, the optimum point

$$(v_c, \beta_c) = (0.04, 2.96+), \quad (47)$$

as the most likely place for our civilization, lies right on the critical curve (see Fig. 10). This situation is unstable: a small decrease in β transfers civilization to the stable area where the population eventually reaches a plateau of 10.2 – 10.4 billion. On the contrary, with a small increase in β , civilization falls into the unstable area where it disappears over time. Its lifetime depends on the depth of invasion of the unstable area: the farther from the critical curve, the shorter the lifetime (Table 3). So, with $\beta = 2.97$, civilization disappears in 20292, and with $\beta = 3$ much earlier, already in 5127. For the scenarios $\beta = 2.96$ and 2.97, population maximums coincide: 9.3 billion in 2058; minimums are also the same, 7.7 billion, but the years of their appearance are slightly different: 2381 and 2391. The first temperature maximums are the same, 16.4°C; they fall on 2320 and 2341. In the supercritical scenario $\beta = 2.97$, there is a second temperature maximum of 17.1°C, which falls on 20181; and 111 years after that, civilization disappears. In the short term (by the year 2100), both scenarios give a population of 8.9 billion and a temperature of 16.0°C (against the current 15°C).

Let us consider a group of scenarios in the range $v = 0.03 - 0.044$ and $\beta = 2.7 - 3.3$ around the optimum point (v_c, β_c) corresponding to the level $S_{\text{total}} = 1.63\%$ (Fig. 20). They give the following ranges of the population: 9.1 – 9.4 billion in 2050, and 8.5 – 9.3 billion in 2100. The population maximum of 9.1 – 9.5 billion appears in the interval 2054 – 2062. All scenarios from this group give the same temperature in the corresponding year: 15.4°C in 2050 and 16.0°C in 2100. In other scenarios, the variables change as shown in Fig. 13.

Note that there are no intermediate stable states: the population either reaches the upper plateau or vanishes. So, we can conclude that civilization is at the edge of stability.

Relations (45) and the obtained values of v and β allow us to find the temperature tolerance and the scale of mortality responsible for the loss of knowledge: $\sigma = 1.14$ K and $m_s = 0.032$

billion/year. If instead of the population scale N_s in the definition of m_s we use the current population $N = 7.7$ billion, then we get $m = 0.046$ billion/year.

Let us compare m with real mortality. It is known (UN, 2019) that crude death rate is now 7.6 per 1000 per year that yields mortality $m_0 = 0.059$ billion/year. The inequality $m < m_0$ means that knowledge is lost more slowly than knowledge holders die, which can be explained by the transfer of knowledge to the next generations through learning. Otherwise, when $m > m_0$, knowledge is lost faster than holders die; this may be, for example, due to problems with education.

The wider and better the education, the smaller the m (and also the m_s). Accordingly, the loss coefficient v also decreases, so that with the same temperature sensitivity β , civilization deepens into the stable area (Fig. 10), which confirms the well-known truth: improving education increases the stability of civilization. On the contrary, with degrading education, the coefficient v increases, and civilization shifts to the area of instability. Thus, the control parameter v reflects the capabilities of the education system as a knowledge dissemination tool. This opens up the possibility of expanding our model in two ways: (i) by including in the model a dynamic equation for v which describes processes in the education system; or (ii) by introducing an objective functional depending on v , and then solving the optimization problem. Meanwhile, in this study, the parameter v is constant throughout a scenario but changes when moving from one scenario to another.

8. Conclusion

A model of the civilization–environment system has been developed, in which the dynamics of the following macro-variables are tracked: world population, the amount of knowledge used, the share of fossil fuels in world energy consumption, CO₂ concentration in the atmosphere, and global mean surface temperature. Distinctive features of this model are as follows. The equation for knowledge production rate takes into account energy dissipation and its relationship with CO₂ concentration and temperature. The concept of active knowledge circulating in society and determining the level of life-support technologies is introduced in the model. Knowledge is produced by humanity (which acts as a combination of producers and holders of knowledge) at a rate proportional to the population. At the same time, knowledge is lost due to mortality at a rate inverse to the population. The CO₂ balance equation considers emissions from burning fossil

fuels and also reverse processes — land uptake and ocean invasion. The dependence of CO₂ emissions on the population and the amount of active knowledge has been established.

The model developed was calibrated using literature data for all calculated variables. In calibration, two control parameters remained free: knowledge loss coefficient ν and sensitivity of population to temperature rise β , which determine all other model parameters. Scenarios corresponding to different values of the control parameters well consistent with historical data but give different trends in the future. In total, about 90 scenarios were calculated.

It was found that in space (ν, β) there are two areas separated by the critical curve $\beta(\nu)$: one corresponds to sustainable development, and the other to loss of stability. Calculations show that the total deviation of the model from empirical data reaches a minimum for the scenario which corresponds to the point $(\nu, \beta) = (0.04, 2.96+)$ located right on the critical curve. This point determines the most probable state of our civilization. Location on the critical curve is unstable: a small deviation can eventually lead to either stabilization of the population at the level of 10+ billion, or the complete extinction of civilization. There are no intermediate steady states.

Analysis of various scenarios shows that until 2100 it is already difficult to change the dynamics of temperature rise due to the inertia of the world economy since the share of fossil fuels in energy consumption decreases very slowly: 85% at present, ~70% by the mid-century, and ~40% by the end-century.

The model shows the danger of a high loss of knowledge since this affects the development of environment-friendly life-support technologies and can lead to the extinction of civilization. Sustainable development is possible only at a sufficiently low knowledge loss, which can be achieved by improving public education.

It is worth emphasizing that the main result of this study is not so much a quantitative prediction of the future, the accuracy of which is unclear because of the unavoidable sketchiness of the model, as a qualitative picture revealing the interconnection of different factors and showing trends in the development of civilization. An important conclusion is that civilization is at the edge of stability.

The approach proposed may also be useful as part of the scenario planning technique for the future, the main idea of which was expressed by Robert Costanza:

“Predicting the future is impossible. But what we can do is layout a series of plausible scenarios,

which help to better understand future possibilities and the uncertainties surrounding them.” (Costanza, 2013).

Conflicts of interest: The author declares no conflict of interest.

References

- Akaev A.A, Sadovnichii, V.A., 2010. Mathematical model of population dynamics with the world population size stabilizing about a stationary level. *Dokl. Math.* 82 (3), 978–981.
- Andrews, O., Le Quéré, C., Kjellstrom, T., Lemke, B., Haines, A., 2018. Implications for workability and survivability in populations exposed to extreme heat under climate change: a modelling study. *Lancet Planet Health* 2, e540–47.
- Aral, M.M., 2013. Climate change and human population dynamics. *J. Water Qual. Exp. Health* 6, 53–62. <http://dx.doi.org/10.1007/s12403-013-0091-5>.
- Aral, M.M., 2014. Climate change and persistent high temperatures: does it matter? *J. Front. Environ. Sci.* 2 (45), 1–8. <http://dx.doi.org/10.3389/fenvs.2014.00045>.
- Archer, D., Eby, M., Brovkin, V., Ridgwell, A., Cao, L., Mikolajewicz, U., Caldeira, K., Matsumoto, K., Munhoven, G., Montenegro, A., Tokos, K., 2009. Atmospheric lifetime of fossil fuel carbon dioxide. *Annu. Rev. Earth Planet. Sci.* 37, 117–134.
- BP, 2018. <https://www.bp.com/en/global/corporate/energy-economics/statistical-review-of-world-energy.html>
- Burch, T.K., 2015. Error in demographic and other quantitative data and analyses. In: *Population Change and Lifecourse Strategic Knowledge Cluster Discussion Paper Series* 3 (3), Article 1. <http://ir.lib.uwo.ca/pclc/vol3/iss3/1>
- Burgin, M., 2017. *Theory of Knowledge: Structures and Processes*, World Scientific.
- Costanza, R., 2013. A theory of socio-ecological system change. *Journal of Bioeconomics*. DOI 10.1007/s10818-013-9165-5.
- Dolgonosov, B.M., Naidenov, V.I., 2006. An informational framework for human population dynamics. *Ecological Modelling* 198, 375–386.

- Dolgonosov, B.M., 2009. *Nonlinear Dynamics of Ecological and Hydrological Processes*. Moscow: Librokom, 440 pp. (in Russian).
- Dolgonosov, B.M., 2016. Knowledge production and world population dynamics. *Technological Forecasting & Social Change* 103, 127–141.
- Dolgonosov, B.M., 2018. A conceptual model of the relationship among world economy and climate indicators. *BioPhysical Economics and Resource Quality* 3:4.
- Dong, J., Li, W., Cao, Y., Fang, J., 2016. How does technology and population progress relate? An empirical study of the last 10,000 years. *Technological Forecasting & Social Change* 103, 57–70.
- Ghirlanda, S., Enquist, M., Perc, M., 2010. Sustainability of culture-driven population dynamics. *Theoretical Population Biology* 77, 181–188.
- Hilbert, M., López, P., 2012a. How to measure the world's technological capacity to communicate, store, and compute information? Part I: results and scope. *International Journal of Communication* 6, 956–979.
- Hilbert, M., López, P., 2012b. How to measure the world's technological capacity to communicate, store, and compute information? Part II: measurement unit and conclusions. *International Journal of Communication* 6, 936–955.
- IAC Switzerland, 2014. <https://www.co2.earth/historical-co2-datasets>
- IPCC, 1990. <https://www.ipcc.ch/report/ar1/wg1/>
- IPCC, 2013. <https://www.ipcc.ch/report/ar5/wg1/>
- Joos, F., Roth, R., Fuglestedt, J.S., Peters, G.P., Enting, I.G., von Bloh, W., Brovkin, V., Burke, E.J., Eby, M., Edwards, N.R., Friedrich, T., Frölicher, T.L., Halloran, P.R., Holden, P.B., Jones, C., Kleinen, T., Mackenzie, F.T., Matsumoto, K., Meinshausen, M., Plattner, G.-K., Reisinger, A., Segschneider, J., Shaffer, G., Steinacher, M., Strassmann, K., Tanaka, K., Timmermann, A., Weaver, A.J., 2013. Carbon dioxide and climate impulse response functions for the computation of greenhouse gas metrics: a multi-model analysis. *Atmos. Chem. Phys.* 13, 2793–2825.
- Library of Congress, 2017. <https://www.loc.gov/about/reports-and-budgets/annual-reports/>

Miranda, L.C.M., Lima, C.A.S., 2011. On the forecasting of the challenging world future scenarios. *Technological Forecasting & Social Change* 78, 1445–1470.

NASA, 2016. GISS. https://data.giss.nasa.gov/gistemp/tabledata_v3/GLB.Ts+dSST.txt

Okuducu, M.B., Aral, M.M., 2017. Knowledge based dynamic human population models. *Technological Forecasting & Social Change* 122, 1–11.
<http://dx.doi.org/10.1016/j.techfore.2017.05.008>.

Parolari, A.J., Katul, G.G., Porporato, A., 2015. The Doomsday Equation and 50 years beyond: new perspectives on the human-water system. *WIREs Water*. doi: 10.1002/wat2.1080.

Puliafito, S.E., Puliafito, J.L., Conte Grand, M., 2008. Modeling population dynamics and economic growth as competing species: An application to CO₂ global emissions. *Ecological Economics* 65, 602 – 615.

Scripps UCSD, 2017. Atmospheric CO₂ data.
http://scrippsco2.ucsd.edu/data/atmospheric_co2/

Solomon, S., Qin, D., Manning, M., Chen, Z., Marquis, M., Tignor, K.B.M., Miller, H.L. (eds), 2007. *Climate change 2007: The physical science basis. Contribution of working group I to the fourth assessment report of the intergovernmental panel on climate change*. Cambridge University Press, Cambridge, 996 pp.

Stutz, A.J., 2014. Modeling the pre-industrial roots of modern super-exponential population growth. *PLoS ONE*, 9(8): e105291. doi:10.1371/journal.pone.0105291

Taagepera, R., 2014. A world population growth model: Interaction with Earth's carrying capacity and technology in limited space. *Technological Forecasting and Social Change* 82, 34–41.

ten Berge, T., van Hezewijk, R., 1999. Procedural and declarative knowledge: an evolutionary perspective. *Theory & Psychology* 9(5), 605–624.

UN, 2019. World population prospects.
<https://population.un.org/wpp/Download/Standard/Population/>

US Census Bureau, 2018. <https://www.census.gov/programs-surveys/international-programs.html>

von Foerster, H., Mora, P.M., Amiot, L.W., 1960. Doomsday: Friday, 13 November, A.D. 2026. *Science* 132, 1291–1295.

Wigley, T.M.L., 1987. Relative contributions of different trace gases to the greenhouse effect. *Climate Monitor* 16, 14–29.

Wiig, K., 1993. *Knowledge Management Foundations: Thinking about Thinking — How People and Organizations Create, Represent, and Use Knowledge*. Schema Press, Arlington, TX.

About the author:

Boris M. Dolgonosov, Ph.D. (1979, Moscow State University), D.Sc. (1997, Russian Academy of Sciences), head of the Ecological modeling laboratory, Institute of Water Problems, Russian Academy of Sciences, Moscow — until September 2014. Currently: Independent researcher, Haifa, Israel; the author of more than 160 scientific publications and two monographs.